#1430

Reprinted from the Soil Science Society of America Journal
Volume 60, no. 2, March-April 1996
677 South Segoe Rd., Madison, WI 5371 1 USA

Convective-Dispersive Stream Tube Model for Field-Scale Solute Transport: I. Moment Analysis

Nobuo Toride and Feike J. Leij*

ABSTRACT

Field-scale solute transport is typically difficult to model due to the complexity and heterogeneity of flow and transport in natural soils. The stream tube model attempts to stochastically describe transport across the field for relatively short travel distances by viewing the field as a series of independent vertical soil columns. This study investigates the stream tube model with the chemical equilibrium and nonequilibrium convection-dispersion equation (CDE) for local-scale transport. A bivariate (joint) lognormal probability density function was used for three pairs of random transport parameters: (i) the dispersion coefficient, D, and the pore-water velocity, v; (ii) the distribution coefficient for linear adsorption, K_d, and v; and (iii) the first-order rate coefficent for nonequilibrium adsorption, a, and v. Expressions for travel time moments as a rsult of a Dirac input were derived to characterize field-scale transport according to the stream tube model. The mean breakthrough time for the field-scale flux-averaged concentration, $\hat{c}_f$, was found to be identical to that for the deterministic CDE. Variability in D has generally a minor effect on solute spreading compared with variability in v. Spreading of reactive solutes increased for negatively correlated v and K_d, even if the variability in K_d was relatively small, while nonequilibrium adsorption further increased spreading. If a was variable, a negative correlation between v and a enhanced the skewness of the breakthrough curve for&while spreading was independent of the correlation between α and v.

FIELD-SCALE SOLUTE TRANSPORT has been the topic of considerable experimental and theoretical research because of concerns for the quality of the subsurface environment, which is especially threatened by downward movement of contaminants. Traditional deterministic modeling approaches, based upon the CDE for chemical transport and the Richards equation for water flow, work relatively well for homogeneous field soils and packed laboratory columns. Experimental investigations, however, have shown that flow and transport processes in most fields are heterogeneous (Biggar and Nielsen, 1976; Sudicky, 1986).

Three approaches may be employed to describe field-scale transport (Jury and Fltihler, 1992): (i) the traditional convective-dispersive model; (ii) a stochastic-continuum model that uses covariance functions for random local-scale transport parameters (e.g., Dagan, 1984; Kabala and Sposito, 1991; Sposito and Barry, 1987); and (iii) a stochastic-convective stream tube model that views the field as a series of independent vertical soil columns (Dagan, 1993; Jury and Roth, 1990). These models are distinguished by the degree of lateral solute mixing (Jury and Fltihler, 1992). The stream tube model does not allow horizontal mixing, and the concentration for each tube represents a discrete value in the horizontal plane. On the other hand, the CDE assumes perfect mixing, and the concentration across the horizontal plane is uniform for one-dimensional, vertical transport. During field-scale transport, it is likely that a transition occurs from a stochastic-convective to a convective-dispersive process.

Dagan and Bresler (1979) and Bresler and Dagan (1979) first described downward movement of nonreactive solutes at the field scale with the stream tube model. They assumed a lognormal distibution for the saturated hydraulic conductivity. Amoozegar-Fard et al. (1982) demonstrated the effect of a random pore-water velocity, v, and dispersion coefficient, D, on field-scale concentrations with Monte Carlo simulation. Jury (1982) proposed a CLT, which neglects local-scale dispersion. Van der Zee and van Riemsdijk (1986, 1987) applied the stream tube model to reactive solutes, while Destouni and Cvetkovic (1991) introduced physical and chemical nonequilibrium in the local-scale transport model. Jury and Scotter (1994) discussed the application of the stochastic-convective model to boundary and initial value problems. They pointed out that stochastic stream tube models have not been used as widely as convective-dispersive and stochastic-continuum models due to the limited discussion of its theoretical foundation and a lack of procedures for its application.

The purpose of this study is to further investigate field-scale transport with the stream tube model for reactive and nonreactive solutes. The effect of the variability in local-scale transport parameters on field-scale solute transport is demonstrated by obtaining field-scale mean concentrations with the chemical nonequilibrium or equilibrium formulation of the CDE for local-scale transport. Three pairs of random transport parameters are used, which are described with a bivariate lognormal pdf: the pore water velocity, v ($cm\ d^{-1}$), in combination with either the dispersion coefficient, D ($cm^2\ d^{-1}$), the distribution coefficient for linear adsorption, K_d ($cm^3\ g^{-1}$), or the first-order rate coefficient for nonequilibrium adsorption, a (d^{-1}). The volumetric water content, θ ($cm^3\ cm^{-3}$), and the soil bulk density, ρ_b ($g\ cm^{-3}$), are always assumed to be deterministic. Since we use a linear CDE for local-scale transport, the resulting stream tube model for field transport is also linear. Hence, we can derive moments of the travel time pdf to characterize field-scale solute distributions. Several typical examples of resident concentration profiles and field-scale BTC will be discussed with time moments. In the second part of this study (Toride and Leij, 1996), the stream tube model is applied to various types of boundary and initial value problems that may occur in the field.

N. Toride, Dep. of Agricultural Sciences, Saga Univ., Saga 840, Japan; and F.J. Leij, U.S. Salinity Lab., 450 West Big Spring Road, Riverside, CA 925074617. Contribution from the USDA-ARS Salinity Laboratory. Received 28 July 1994. *Corresponding author (fleij@ussl.ars.usda.gov).

Published in Soil Sci. Soc. Am. J. 60:342-352 (1996).

Abbreviations: BTC, breakthrough curve; CDE, convection-dispersion equation; CLT, convective lognormal transer function model; CV, coefficient of variation; pdf, probability density function.

MODEL

Local-Scale Transport

Solute transport in a local-scale stream tube is described with the one-dimensional CDE. For steady downward flow and first-order kinetic linear adsorption, the CDE is given by

$$\frac{\partial c_r}{\partial t} + \frac{\rho_b}{\theta}\frac{\partial s}{\partial t} = D\frac{\partial^2 c_r}{\partial x^2} - v\frac{\partial c_r}{\partial x} \quad [1]$$

$$\frac{\partial s}{\partial t} = \alpha(K_d c_r - s) \quad [2]$$

where c_r is the volume-averaged (resident) concentration (g cm^{-3}), s is the concentration of the adsorbed phase (g g^{-1}), x is depth (cm), and t is time (d). The nonequilibrium CDE reduces to the conventional CDE for instantaneous adsorption ($\alpha \to \infty$):

$$R\frac{\partial c_r}{\partial t} = D\frac{\partial^2 c_r}{\partial x^2} - v\frac{\partial c_r}{\partial x} \quad [3]$$

where the retardation factor R is given by

$$R = 1 + \frac{\rho_b K_d}{\theta} \quad [4]$$

For instantaneous solute application to a soil that is initially solute free, the initial and boundary conditions for both the equilibrium and nonequilibrium CDE may be written as

$$c_r(x,0) = s(x,0) = 0 \quad [5]$$

$$vc_r(0,t) - D\frac{\partial c_r(0,t)}{\partial x} = m_B\delta(t) \quad [6]$$

$$\frac{\partial c_r}{\partial x}(\infty,t) = 0 \quad [7]$$

where $\delta(t)$ is the Dirac delta function (d^{-1}), and m_B is the amount of mass added to a unit area of soil solution (g cm^{-2}). The following analytical solution for Eq. [1] and [2] subject to Eq. [5] through [7] can be derived with the help of Laplace transforms (Lindstrom and Narasimhan, 1973; Jury and Roth, 1990; Toride et al., 1993):

$$c_r(x,t) = \frac{m_B}{v}\left[\Gamma(x,t;R'=1)\exp\left(-\frac{\alpha\rho_b K_d t}{\theta}\right) + \alpha\sqrt{\frac{\rho_b K_d}{\theta}}\int_0^t\sqrt{\frac{\tau}{t-\tau}}\,\Gamma(x,\tau;R'=1)H_1(\tau)d\tau\right] \quad [8a]$$

$$s(x,t) = \frac{m_B\alpha}{v}\int_0^t \Gamma(x,\tau;R'=1)H_0(\tau)d\tau \quad [8b]$$

where

$$\Gamma(x,\tau;R') = \frac{v}{\sqrt{\pi DR'\tau}}\exp\left[-\frac{(R'x-v\tau)^2}{4DR'\tau}\right] - \frac{v^2}{2DR'}\exp\left(\frac{vx}{D}\right)\mathrm{erfc}\left(\frac{(R'x+v\tau)}{2\sqrt{DR'\tau}}\right) \quad [9]$$

$$H_j(\tau) = \exp\left[-\frac{\alpha\rho_b K_d\tau}{\theta} - a(t-\tau)\right]$$

$$I_j\left[2\alpha\sqrt{\frac{\rho_b K_d(t-\tau)\tau}{\theta}}\right] \quad j = 0, 1 \quad [10]$$

with I_j as the modified Bessel function of order j. These solutions can be simplified for equilibrium adsorption according to

$$c_r(x,t) = \frac{m_B}{v}\Gamma(x,t;R'=R),$$
$$s(x,t) = K_d c_r(x,t) \quad [11a,b]$$

The above solutions are for volume-averaged (resident) concentrations. Flux-averaged or flowing concentrations, c_f, should be used if a solute flux across some observation plane is determined (e.g., effluent curves obtained from finite soil columns). Flux-averaged and resident concentrations are related through the transformation (Kreft and Zuber, 1978):

$$c_f = \frac{J_s}{J_w} = c_r - \frac{D}{v}\frac{\partial c_r}{\partial x} \quad [12]$$

where J_s is the solute flux density (g cm^{-2} d^{-1}), and J_w is the water flux density (cm^3 cm^{-2} d^{-1}). Substituting the solutions for c_r into Eq. [12] results in a mathematically identical set of equations for c_f, i.e., Eq. [8a] and [8b] for the nonequilibrium CDE and Eq. [11a] and [11b] for the equilibrium CDE, but $\Gamma(x,t;R')$ is now given by (Toride et al., 1993):

$$\Gamma(x,\tau;R') = \frac{x}{2}\sqrt{\frac{R'}{\pi D\tau^3}}\exp\left[-\frac{(R'x-v\tau)^2}{4DR'\tau}\right] \quad [13]$$

The solutions for a Dirac input with $m_B/v = 1$ are often referred to as the travel time pdf or the residence time distribution, $f(x,t)$. The solution for an arbitrary input function, $g(t)$, can be readily obtained from this special case with the convolution

$$c_r(x,t) = \int_0^t g(t-\tau)f(x,\tau)d\tau \quad [14]$$

Once the independent variables, t and x, are specified, the solutions of the local-scale transport equation can be viewed to solely depend on the values of transport parameters such as v, D, and K_d. As an example, Fig. 1a shows the solution for the equilibrium CDE, c_r, for a pulse input of 2 d, as a function of v and K_d at x = 100 cm and t = 5 d with D = 20 cm^2 d^{-1} and ρ_b/θ = 4 g cm^{-3}. As K_d increases, the solute moves slower through the medium because of increased adsorption; a higher v is required for the solute to reach the same position (x = 100 cm) after 5 d. Figure 1b and 1c will be discussed further in the text. In the following, we will always use normalized concentrations. For a Dirac input, m_B/v is assumed to be equal to unity; the dimensional and normalized concentrations are identical and any consistent set of units can be used for c.

Field-Scale Transport

Bivariate Lognormal Distribution

A bivariate lognormal pdf will be used for the two random parameters in the deterministic model for transport in each stream tube. The lognormal distribution is often used to describe skewed as well as symmetrical pdf. We assume θ and ρ_b to be the same for all stream tubes since the CV for these two parameters is generally much lower than the CV for the

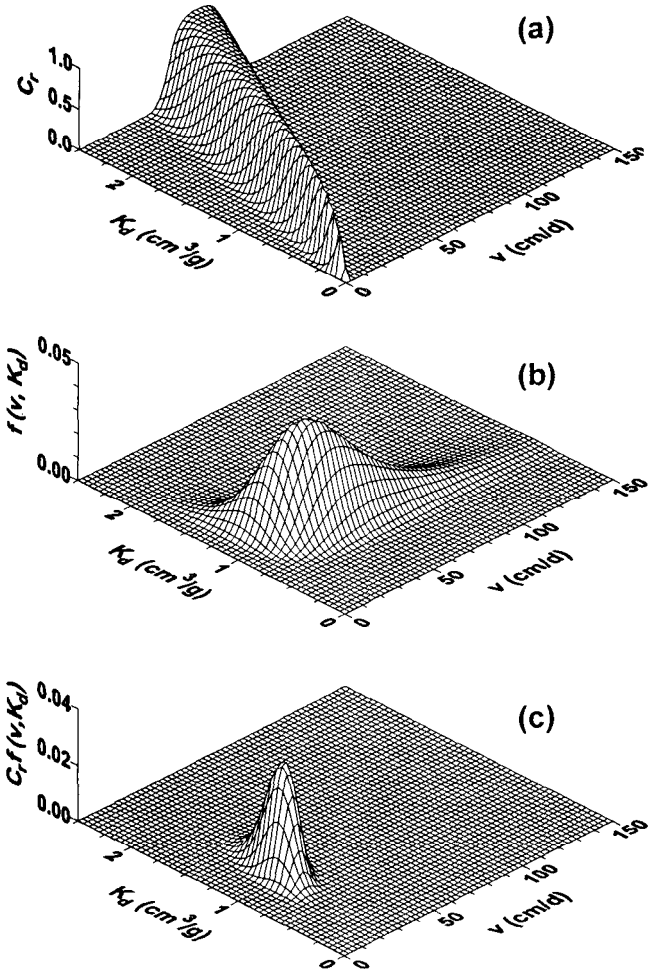

Fig. 1. The stochastic convective-dispersive stream-tube model for a variable pore-water velocity, v, and distribution coefficient, K_d: (a) local-scale resident concentration, c_r, for a pulse input of 2 d as a function of v and K_d at depth, x = 100 cm, and time, t = 5 d; (b) a bivariate lognormal probability density function (pdf) for the correlation coefficient, ρ_{vK_d} = -0.5; and (c) expected c_r at x = 100 cm and t = 5 d as obtained by multiplying c_r in (a) by the pdf in (b).

hydraulic conductivity (Jury et al., 199 1). The heterogeneity of the flow field is entirely characterized by the pdf for the pore-water velocity, v. The general bivariate lognormal pdf can be defined as (Spiegel, 1992, p. 118)

$$f(v,\eta) = \frac{1}{2\pi\sigma_v\sigma_\eta v\eta\sqrt{1-\rho_{v\eta}^2}} \exp\left(-\frac{Y_v^2 - 2\rho_{v\eta}Y_vY_\eta + Y_\eta^2}{2(1-\rho_{v\eta}^2)}\right) \quad [15]$$

with

$$Y_v = \frac{\ln(v)-\mu_v}{\sigma_v}, \quad Y_\eta = \frac{\ln(\eta)-\mu_\eta}{\sigma_\eta} \quad [16a,b]$$

$$\rho_{v\eta} = \langle Y_vY_\eta\rangle = \int_0^\infty\int_0^\infty Y_vY_\eta f(v,\eta)\,dv\,d\eta \quad [17]$$

where η denotes D, K_d, or a (i.e., the random parameter in addition to v), μ and σ are the mean and standard deviation of the log-transformed variables, and $\rho_{v\eta}$ is the coefficient of

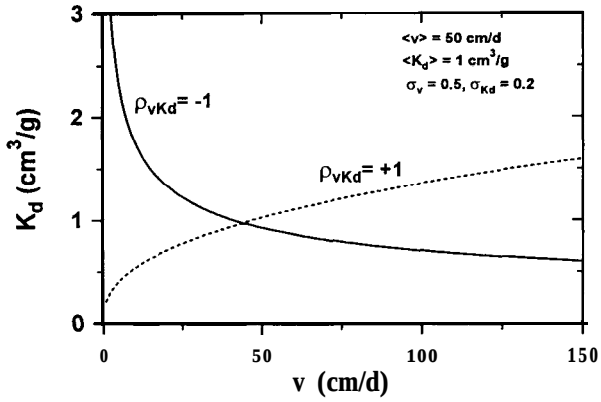

Fig. 2. The stochastic distribution coefficient, K_d, vs. pore-water velocity, v, for a perfect negative ($\rho_{vK_d} = -1$) and positive ($\rho_{vK_d} = 1$) correlation.

correlation between Y_v and Y_η. The ensemble averages of v and η are (Aitcheson and Brown, 1963, p. 8)

$$\langle v\rangle = \exp\left(\mu_v + \frac{1}{2}\sigma_v^2\right), \quad \langle\eta\rangle = \exp\left(\mu_\eta + \frac{1}{2}\sigma_\eta^2\right) \quad [18a,b]$$

and the coefficient of variation CV is

$$\mathrm{CV}(v) = \sqrt{\exp(\sigma_v^2) - 1},$$
$$\mathrm{CV}(\eta) = \sqrt{\exp(\sigma_\eta^2) - 1} \quad [19a,b]$$

Figure lb presents an example of a bivariate lognormal pdf for v and K_d, $f(v,K_d)$, with $\langle v\rangle$ = 50 cm d^{-1}, σ_v = 0.2, $\langle K_d\rangle$ = 1 cm^3 g^{-1}, σ_{K_d} = 0.2, and ρ_{vK_d} = -0.5. The distribution in terms of v is **skewed** due to the relatively high standard deviation, σ_v, whereas the smaller σ_{K_d} results in a more symmetric distribution in terms of K_d. One may notice that v tends to increase for decreasing K_d as a result of the negative ρ_{vK_d}.

The joint pdf given by Eq. [15] can be simplified for particular values for $\rho_{v\eta}$. The joint pdf becomes equal to the product of two univariate lognormal distributions when the two parameters are uncorrelated ($\rho_{v\eta} = 0$):

$$f(v,\eta) = f(v)f(\eta) \quad [20]$$

where the univariate lognormal distribution is given by

$$f(\eta) = \frac{1}{\sqrt{2\pi}\sigma_\eta\eta}\exp\left(-\frac{[\ln(\eta)-\mu_\eta]^2}{2\sigma_\eta^2}\right) \quad [21]$$

Perfect correlation leads to $Y_\eta = Y_v$ ($\rho_{v\eta} = 1$) and $Y_\eta = -Y_v$ ($\rho_{v\eta} = -1$), respectively. Subsequent use of Eq. [18a] and [18b] yields an expression of η in terms of v:

$$\eta(v) = \left(\frac{v}{\langle v\rangle}\right)^{\rho_{v\eta}\sigma_\eta/\sigma_v}\langle\eta\rangle\exp\left(\frac{\rho_{v\eta}}{2}\sigma_v\sigma_\eta - \frac{1}{2}\sigma_\eta^2\right) \quad [22]$$

Figure 2 demonstrates the two cases of perfect correlation between v and K_d with the same values for the mean and standard deviation as in Fig. lb for the bivariate lognormal distribution. For a perfect negative correlation ($\rho_{vK_d} = -1$), K_d decreases as v increases while the opposite is true for a positive correlation when $\rho_{vK_d} = 1$.

Field-Scale Mean Concentration

In the stochastic stream tube model, field-scale transport during steady state downward water flow is described by averaging local-scale concentrations across all stream tubes.

The spatial average for the entire field is assumed equal to the ensemble average:

$$\langle c(x,t)\rangle = \frac{1}{A}\int_A c(x,t)\,dA = \int_0^\infty\int_0^\infty c_r(x,t;v,\eta)f(v,\eta)\,dv\,d\eta \quad [23]$$

where A denotes the area of the field. The ensemble average of the local concentration can be defined both for the flux-averaged ($\langle c_f\rangle$) and the resident ($\langle c_r\rangle$) modes.

The field-scale resident concentration, $\hat{c}_r$, i.e., c_r averaged across the entire horizontal plane at a particular depth, is defined as the ensemble average, $\langle c_r\rangle$, given by Eq. [23]. Figure lc shows the product of the concentration distribution (Fig. la) and the joint pdf (Fig. lb) as an example of the integrand on the right side in Eq. [23]. The peak of the plot in Fig. lc indicates that stream tubes for which v is ≈ 25 cm d^{-1} and K_d is $\approx 1\ cm^3 g^{-1}$ contribute the most to the field-scale mean concentration at $x = 100$ cm and $t = 5$ d. The total volume of the distribution in Fig. lc corresponds to the ensemble average of c_r, and hence the field-scale concentration, $\hat{c}_r$. The field-scale total resident concentration $\hat{c}_T$ quantifies the amount of solute in the liquid and adsorbed phases per volume of solution:

$$\hat{c}_T = \left\langle c_r + \frac{\rho_b s}{\theta}\right\rangle = \hat{c}_r + \frac{\rho_b}{\theta}\langle s\rangle \quad [24]$$

The field-scale flux-averaged concentration, $\hat{c}_f$, can be defined **in a similar manner as** Eq. [12] as the ratio of the mean solute and water fluxes:

$$\hat{c}_f(x,t) = \frac{\langle vc_f\rangle}{\langle v\rangle} = \frac{\int_0^\infty\int_0^\infty vc_f(x,t;v,\eta)f(v,\eta)\,dv\,d\eta}{\langle v\rangle} \quad [25]$$

The solute flux for an entire field is given by $A\theta\langle v\rangle\hat{c}_f$. To evaluate $\hat{c}_f$, it is necessary to determine the local-scale v and c_f (at the same location). Note that $\hat{c}_f$ is different from $\langle c_f\rangle$ for a stochastic v since, in general, $\langle vc_f\rangle \neq \langle v\rangle\langle c_f\rangle$. If local values for v cannot be easily obtained, the pdf for the pore water **velocity**, $f(v)$, may be estimated from solute displacement data by applying Eq. [23] to either $\hat{c}_r = \langle c_r\rangle$ or $\langle c_f\rangle$. Once f(v) is specified, $\hat{c}_f$ can be used to predict the field-scale solute flux.

Values for the field-scale mean concentration were obtained by substituting analytical solutions for the local-scale CDE and the joint pdf into Eq. [23] or [25]. Numerical integration was carried out on the log-transformed v and η with Romberg quadrature. Analytical solutions for the local-scale CDE were evaluated as described by Toride et al. (1993). The accuracy and efficiency of the numerical integration was also improved by narrowing the integration limits for v and η by excluding improbable values. The computer program for evaluating the above local- and field-scale transport problems is described by **Toride** et al. (1995).

Time Moment **Analysis**

Time moments of the BTC in terms of the concentration given by Eq. [23] and [25] are useful to characterize transport behavior. The nth normalized time moment, M_n, for an arbitrary concentration mode can be defined as (Leij and Dane, 1991)

$$M_n(x;c) = \frac{m_n}{m_0} = \frac{\int_0^\infty t^n c(x,t)\,dt}{\int_0^\infty c(x,t)\,dt} \quad [26]$$

where m_n represents the nth regular time moment with $m_0 = m_B/v$ for a Dirac delta input in Eq. [6]. Substitution of Eq. [23] into Eq. [26] yields the time moments for $\hat{c}_r$ or $\langle c_r\rangle$, and $\langle c_f\rangle$:

$$M_n(x;\langle c\rangle) = \frac{1}{m_0}\int_0^\infty t^n\left[\int_0^\infty\int_0^\infty c(x,t;v,\eta)\,f(v,\eta)\,dv\,d\eta\right]dt$$
$$= \int_0^\infty\int_0^\infty M_n^{loc}(x;c)\,f(v,\eta)\,dv\,d\eta \quad [27]$$

where M_n^{loc} is the **nth** normalized time moment for the local-scale CDE, and m_0 ($= m_B/v$) is a deterministic constant for all stream tubes. Note that m_B **is** proportional to the stochastic parameter v for the flux-mode injection (Eq. [16]). The order of integration in Eq. [27] can be changed because the pdf is time invariant. Similarly, time moments for $\hat{c}_f$ are obtained by substituting Eq. [25] into Eq. [26] to obtain

$$M_n(x;\hat{c}_f) = \frac{1}{m_0\langle v\rangle}\int_0^\infty\int_0^\infty vM_n^{loc}(x;c_f)\,f(v,\eta)\,dv\,d\eta \quad [28]$$

The first (M_1^{loc}) and second (M_2^{loc}) normalized local time moments of c_f and c_r for the nonequilibrium CDE with a Dirac input are presented in Table 1 (Valocchi, 1985). The nth time moment can be derived from solutions in the **Laplace** domain according to

$$m_n^{loc}(x;c) = (-1)^n \lim_{p\to 0}\left[\frac{d^n}{dp^n}\bar{c}(x,p)\right] \quad [29]$$

where $\bar{c}(x,p)$ is the Laplace transform of $c(x,t)$ with respect to time, and p is the corresponding transform variable. Moments for the equilibrium CDE are obtained by letting $\alpha\to\infty$. Normalized time moments for the field-scale mean concentration are derived by substituting the local normalized moments, M_n^{loc}, of Table 1 into Eq. [27] or [29]. The ensemble average of the ratio of two stochastic parameters is evaluated according to Eq. [A3] of the Appendix.

RESULTS AND DISCUSSION

Time Moments

Table 2 presents two time moments of the field-scale flux-averaged concentration, $\hat{c}_f$, in terms of parameters of the bivariate lognormal distribution, $f(v,D)$, $f(v,K_d)$, **and** $f(v,\alpha)$, as given by Eq. [15]. The first moment, M_1, describes the mean breakthrough time, while the second

Table 1. **Normalized first (M_1^{loc}) and second (M_2^{loc}) time moments of the flux (c_f) and resident (c_r) concentration for the nonequilibrium convection-dispersion equation as a result of a Dirac input.†**

Concentration	M_1^{loc}	M_2^{loc}
c_f	$\frac{RX}{v}$	$\frac{2(R-1)x}{\alpha v} + \frac{2DR^2x}{v^3} + \frac{R^2x^2}{v^2}$
c_r	$\frac{DR}{v^2} + \frac{Rx}{v}$	$\frac{2(x + D/v)(R-1)}{\alpha v} + \frac{4D^2R^2}{v^4} + \frac{4DR^2x}{v^3} + \frac{R^2x^2}{v^2}$

† See text **for** definitions of variables.

Table 2. Mean travel time (M_1) and variance (Var_t) of the field-scale flux-averaged concentration, $\hat{c}_f$, as a result of a Dirac delta input with three different probability density functions (pdf).†

Type of pdf	Mean travel time M_1	Variance Var,
$f(v,D)$	$\frac{RX}{\langle v\rangle}$	$\frac{2(R-1)x}{\alpha\langle v\rangle} + \frac{2\langle D\rangle R^2 x}{\langle v\rangle^3}\exp(3\sigma_v^2 - 2\rho_{vD}\sigma_v\sigma_D) + \frac{R^2x^2}{\langle v\rangle^2}[\exp(\sigma_v^2) - 1]$
$f(v,K_d)$	$\frac{\langle R\rangle x}{\langle v\rangle}$	$\frac{2\rho_b\langle K_d\rangle x}{\alpha\theta\langle v\rangle} + \frac{2Dx}{\langle v\rangle^3}\exp(3\sigma_v^2)\left[1 + \frac{2\rho_b\langle K_d\rangle}{\theta}\exp(-2\rho_{vK_d}\sigma_v\sigma_{K_d}) + \frac{\rho_b^2\langle K_d\rangle^2}{\theta^2}\exp(-4\rho_{vK_d}\sigma_v\sigma_{K_d} + \sigma_{K_d}^2)\right] + \frac{x^2}{\langle v\rangle^2}\left\{\exp(\sigma_v^2) - 1 + \frac{2\rho_b\langle K_d\rangle}{\theta}[\exp(\sigma_v^2 - \rho_{vK_d}\sigma_v\sigma_{K_d}) - 1] + \frac{\rho_b^2\langle K_d\rangle^2}{\theta^2}[\exp(\sigma_v^2 - 2\rho_{vK_d}\sigma_v\sigma_{K_d} + \sigma_{K_d}^2) - 1]\right\}$
$f(v,\alpha)$	$\frac{Rx}{\langle v\rangle}$	$\frac{2(R-1)x}{\langle\alpha\rangle\langle v\rangle}\exp(\sigma_\alpha^2) + \frac{2DR^2x}{\langle v\rangle^3}\exp(3\sigma_v^2) + \frac{R^2x^2}{\langle v\rangle^2}[\exp(\sigma_v^2) - 1]$

† See text for definitions of variables.

central moment or variance, $\mathrm{Var}_t(x;\hat{c}_f) = M_2 - M_1^2$, represents the degree of spreading in the solute BTC. The first moment is identical to that for the deterministic CDE (Table 1), except that ensemble averages are used for the random variables. This equivalence indicates that the variability in local parameters does not affect the mean breakthrough in terms of $\hat{c}_f$ at the field scale.

The variance, $\mathrm{Var}_t(x;\hat{c}_f)$, can be partitioned into three different terms for each pdf. As shown in Table 2, the first term is due to nonequilibrium adsorption, the second term is related to local-scale dispersion, D, while the third term is primarily due to velocity differences between the stream tubes (i.e., stochastic convective transport). Similar to the local-scale equilibrium CDE, moments for equilibrium adsorption are obtained by letting $\alpha \to \infty$. The effect of variability in the local parameters on solute spreading can be evaluated by comparing the magnitude of each term in the expression for Var,. For all three pdf, the first and second terms are linear in x whereas the third term in proportional to x^2. Hence, solute spreading due to stochastic-convective transport will become more dominant compared with spreading due to variability in D, K_d, or a, with increasing travel distance, x. Table 2 can also be used to analyze field-scale transport when only one random variable is present by setting the standard deviation for the second random parameter to zero. If both parameters are deterministic, M_1 and Var_t reduce to the expressions given in Table 1. The variance for the deterministic CDE is proportional to x because the third term of Var_t in Table 2 disappears when $\sigma_v = 0$.

A similar moment analysis may be carried out for the mean flux-averaged ($\langle c_f\rangle$) and field-scale resident ($\hat{c}_r = \langle c_r\rangle$) concentrations. We considered the case where only v is a random parameter ($\sigma_\eta = 0$). Table 3 presents the mean breakthrough time, M_1, and variance, Var,, for this simplified scenario. Temporal moments for two random parameters, such as those shown in Table 2 for $\hat{c}_f$, can be easily obtained by Eq. [A3]. The mean breakthrough time, M_1, for $\langle c_f\rangle$ and $\hat{c}_r$ is now affected by the variability in v, in contrast to the mean breakthrough time in terms of $\hat{c}_f$ shown in Table 2. Note that among the three field-scale mean concentrations both MI and Var, are largest for $\hat{c}_r$ and smallest for $\hat{c}_f$.

Nonreactive Solute Transport

To demonstrate the effect of the variability in v and D on field-scale concentrations, we first consider transport of a nonreactive solute ($R = 1$) as described with Eq. [3] at the local scale. Figure 3 shows BTC in terms of $\hat{c}_f$ at $x = 100$ cm when only v is a random variable with three different σ_v and $\langle v\rangle = 50$ cm d^{-1}, and a constant dispersion coefficient, $D = 20$ cm^2 d^{-1}. Deterministic transport occurs when the local-scale velocity is uniform across the field, i.e., $\sigma_v = 0$. The mean travel is 2 d regardless of σ_v (MI in Table 2), while solute spreading increases significantly for greater σ_v. The BTC

Table 3. Mean travel time (M_1) and variance (Var_t) of the mean flux-averaged concentration ($\langle c_f\rangle$) and the field-scale resident concentration ($\hat{c}_r = \langle c_r\rangle$) as a result of a Dirac delta input with a stochastic v.†

Concentration	Mean travel time M_1	Variance Var,
c_r	$\frac{Rx}{\langle v\rangle}\exp(\sigma_v^2)$	$\frac{2(R-1)x}{\alpha\langle v\rangle}\exp(\sigma_v^2) + \frac{2DR^2x}{v^3}\exp(6\sigma_v^2) + \frac{R^2x^2}{\langle v\rangle^2}[\exp(3\sigma_v^2) - \exp(2\sigma_v^2)]$
	$\frac{DR}{\langle v\rangle^2}\exp(3\sigma_v^2) + \frac{Rx}{\langle v\rangle}\exp(\sigma_v^2)$	$\frac{2(R-1)}{\alpha\langle v\rangle}\left[x\exp(\sigma_v^2) + \frac{D}{\langle v\rangle}\exp(3\sigma_v^2)\right] + \frac{D^2R^2}{\langle v\rangle^4}[4\exp(10\sigma_v^2) - \exp(6\sigma_v^2)] + \frac{2DR^2x}{\langle v\rangle^3}[2\exp(6\sigma_v^2) - \exp(4\sigma_v^2)] + \frac{R^2x^2}{\langle v\rangle^2}[\exp(3\sigma_v^2) - \exp(2\sigma_v^2)]$

† See text for definitions of variables.

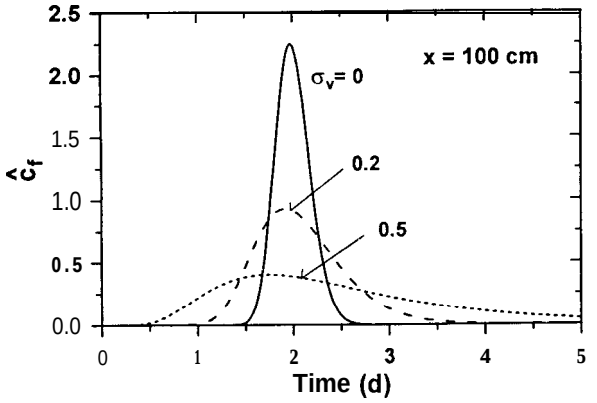

Fig. 3. Field-scale flux-averaged concentrations ($\hat{c}_f$) vs. time for three values of the standard deviation of In v, σ_v, at depth, x = 100 cm, for a nonreactive solute (R = 1).

for σ_v = 0.5 is clearly nonsymmetrical, with early solute breakthrough at the field-scale and significant tailing.

If both v and D are stochastic, a positive correlation between these two parameters is plausible as indicated by the widely used relationship $D = \lambda v$, where λ is the dispersivity (cm). When $\sigma_v = \sigma_D$ and ρ_{vD} = 1, Eq. [22] reduces to ($\eta = D$):

$$D(v) = \frac{\langle D \rangle}{\langle v \rangle} v \qquad [30]$$

This implies that the dispersivity λ is constant (= $\langle D \rangle / \langle v \rangle$) for all stream tubes. If λ is also positively correlated with v, σ_D might be greater than σ_v. Biggar and Nielsen (1976) studied the spatial variability of v and D for a field soil; they found that ρ_{vD} = 0.795, $\langle v \rangle$ = 44.2 cm d^{-1} with σ_v = 1.25, and $\langle D \rangle$ = 367.6 $cm^2 d^{-1}$ with σ_D = 1.74.

Figure 4a presents the travel time variance, Var,, in terms of $\hat{c}_f$ vs. distance. The curves were calculated with the expression for $f(v,D)$ in Table 2 with $\langle v \rangle$ = 50 cm d^{-1} with σ_v = 0.5, and a deterministic (σ_D = 0) or stochastic (σ_D = 0.5, ρ_{vD} = 1) dispersion coefficient where $\langle D \rangle$ is either 20 or 200 cm^2 d-i. The tenfold increase in D resulted in a relatively small increase in the variance, whereas the variability in D ($\sigma_{D = 0.5}$) caused a decrease in the variance for this positive ρ_{vD}. The effect of σ_D on the variance, however, was minor especially for small $\langle D \rangle$ as previously discussed by Amoozegar-Fard et al. (1982) and Bresler and Dagan (1981).

Figure 4b plots the ratio of the third and second terms in the expression for the variance of $\hat{c}_f$, in case of a stochastic v and D (Table 2), vs. travel distance x for the same parameter values as used for Fig. 4a. This ratio is proportional to $\langle v \rangle x / \langle D \rangle$, which may be viewed as the Peclet number in terms of the observation scale, x. Solute spreading due to local-scale dispersion (the second term) is important for small $\langle v \rangle / x / \langle D \rangle$, while spreading due to a stochastic v (the third term) will become dominant for large x, i.e., for increased $\langle v \rangle x / \langle D \rangle$. When $\langle D \rangle$ is small compared with $\langle v \rangle$ (e.g., $\langle v \rangle$ = 50 cm d^{-1} and $\langle D \rangle$ = 20 $cm^2 d^{-1}$ in Fig. 2), the deterministic (σ_D = 0) and stochastic (σ_D = 5)

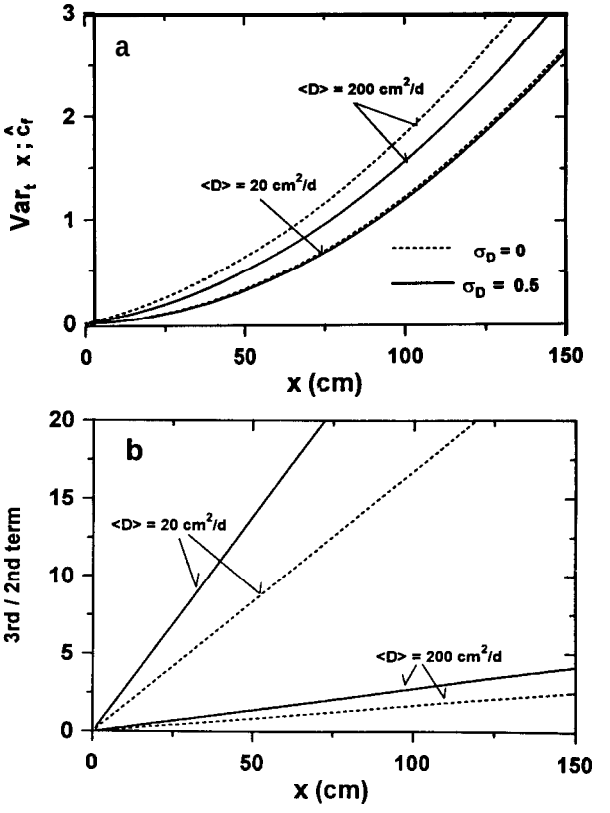

Fig. 4. Travel time variance (Var_t) for field-scale flux-averaged concentrations ($\hat{c}_f$) as a function of travel distance, x, with the local-scale equilibrium convection-dispersion equation for deterministic (σ_D = 0) or stochastic (σ_D = 0.5 and ρ_{vD} = 1) dispersion coefficients, with $\langle D \rangle$ = 20 or 200 $cm^2 d^{-1}$: (a) Var_t profiles, and (b) the ratio of the third to the second terms of Var_t for $f(v,D)$ described in Table 2.

dispersion process will give almost identical results. A constant dispersivity according to Eq. [30] might be appropriate for many applications of the stream tube model where little information is available regarding σ_v and σ_D. This does not imply, however, that local-scale dispersion should be neglected, as will be discussed in the following.

Bresler and Dagan (1981) assumed a local-scale dispersivity , λ, of 3 cm. They concluded that the effect of local-scale dispersion on field-scale concentration profiles is negligible. Most previous studies of stochastic transport have, therefore, neglected local-scale dispersion (Dagan and Cvetkovic, 1993; Destouni and Cvetkovic, 1991; Jury, 1982). As demonstrated in Fig. 4, local-scale dispersion can be neglected for relatively large values of $\langle v \rangle x / \langle D \rangle$. The mean dispersivity observed by Biggar and Nielsen (1976) was 8.3 cm (D = 0.6 + $2.93v^{1.11}$ with ρ_{vD} = 0.795), which exceeds the value of 3 cm used by Bresler and Dagan (1981). Mallants et al. (1996, unpublished data) determined that $D = 31v^{1.93}$ with ρ_{vD} = 0.74 from measurements on undisturbed soil columns of l-m length and 30-cm diameter. These researchers demonstrated that neglecting local-scale dispersion could result in quite different field-scale mean solute distributions. Dispersion coefficients for undisturbed soils are generally much greater than those for repacked soils. For practical applications of the stream

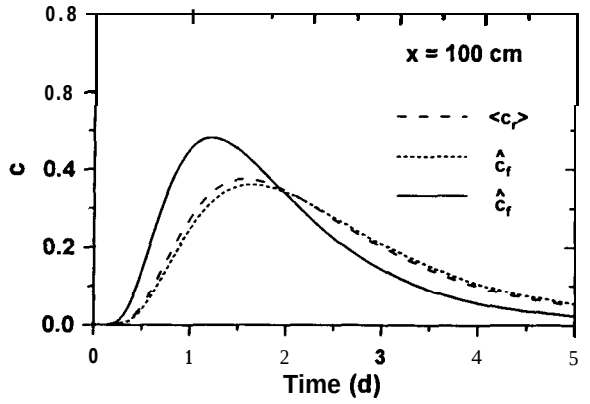

Fig. 5. Breakthrough curves for field-scale flux-averaged ($\hat{c}_f$) and resident ($\hat{c}_r$ = <c_r>) concentrations and ensemble averages of tbe flux-averaged concentration, <c_f>, at x = 100 cm for a nonreactive solute (R = 1).

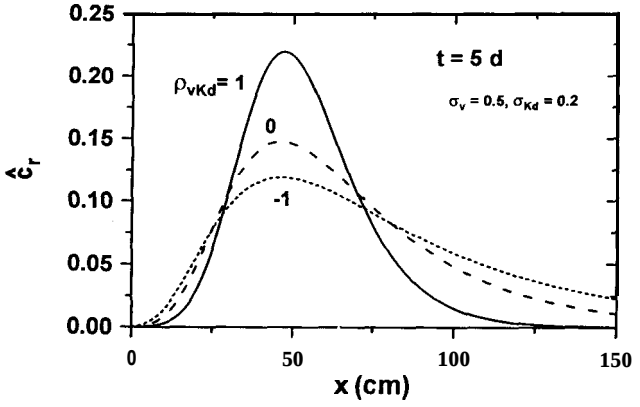

Fig. 7. The effect of correlation between the pore-water velocity and the distribution coefficient, ρ_{vK_d}, on the field-scale resident concentration ($\hat{c}_r$) as a function of depth at time, t = 5 d.

tube model, the value of $<v>x/<D>$ is an index to determine whether or not local-scale dispersion can be neglected (Fig. 4).

Figure 5 presents BTC for three different field-scale concentrations ($\hat{c}_r$, $\hat{c}_f$, and <c_f>) assuming <v> = 50 cm d^{-1} with σ_v = 0.5, and D = 200 $cm^2\ d^{-1}$ with σ_D = 0. The corresponding dispersivity, λ, is 4 cm. The BTC for $\hat{c}_f$ has the highest peak at a relatively early time, while the BTC for $\hat{c}_r$ (= <c_r>) and <c_f> are quite similar. The mean breakthrough time and the amount of spreading are smaller for $\hat{c}_f$ than for $\hat{c}_r$ and <c_f>. This is consistent with the expressions for the time moments in Tables 2 and 3. Notice that the concentration for all modes is almost identical at t = 2 d, which is the mean breakthrough time for $\hat{c}_f$. Since solutes will reach x = 100 cm prior to t = 2 d only in stream tubes with a velocity greater than the ensemble average (<v> = 50 cm d^{-1}), $\hat{c}_f$ according to Eq. [25] is greater than the ensemble-averaged concentrations during the initial stages of the displacement (t < 2 d). On the other hand, $\hat{c}_f$ becomes less than $\hat{c}_r$ or <c_f> for t > 2 d.

Reactive Solute Transport

In addition to variability in v and D, the variability in the distribution coefficient, K_d, and the nonequilibrium rate parameter, a, was also considered for reactive solutes. The effect of a stochastic v or K_d on field-scale concentrations was first investigated for equilibrium adsorption (a-%). Figure 6 shows the travel time variance, Var,, at x = 100 cm for $\hat{c}_f$ as a function of σ_v for five different correlation coefficients, ρ_{vK_d}, with <v> = 50 cm d^{-1}, D = 20 $cm^2\ d^{-1}$, <K_d> = 1 $g^{-1}\ cm^3$, σ_{K_d} = 0.2, <R> = 5, and ρ_b/θ = 4 g cm^{-3}. Figure 6 demonstrates that solute spreading increases for negatively correlated v and K_d in spite of a relatively small value for σ_{K_d}.

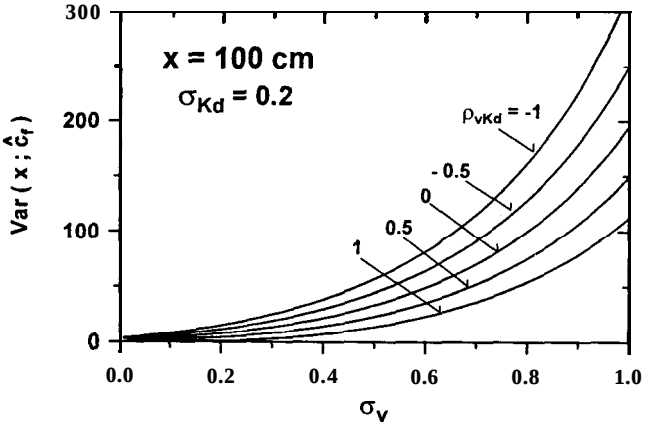

Fig. 6. Travel time variance (Var,) of breakthrough curves for the field-scale flux-averaged concentration ($\hat{c}_f$) at x = 160 cm as a function of σ_v for five correlation coefficients, ρ_{vK_d}.

Figure 7 shows the field-scale resident concentration, $\hat{c}_r$, at t = 5 d as a function of depth for either perfect or no correlation between v and K_d. The same parameter values are used as for Fig. 6. The negative correlation between v and K_d (and hence R) leads to additional spreading of the field-scale concentration. The effect of variability in K_d on solute spreading, with the relatively simple stream tube model, is quite similar as observed from more general stochastic continuum approaches (e.g., Bosma et al., 1993; Cvetkovic and Shapiro, 1990). For relatively high water contents, a negative correlation between v and K_d seems plausible since coarse-textured soils generally have a relatively high conductivity (and hence v) and a small K_d, whereas the opposite is true for fine-textured soils. On the other hand, the unsaturated hydraulic conductivity of fine-textured soils decreases much more rapidly compared with the fine-textured soils as the water content decreases, whereas K_d values would not be greatly influenced by water saturation. Robin et al. (1991) found a weak negative correlation between K_d and the saturated hydraulic conductivity. The sensitivity of the field-scale concentration to σ_{vK_d}, as displayed in Fig. 6 and 7, illustrates the importance of quantifying the relationship between v and K_d.

If solutes are not adsorbed spontaneously, field-scale concentrations can be described with local-scale nonequilibrium transport models such as defined by Eq. [1] and [2]. We will first assume that the nonequilibrium rate parameter, a, is deterministic. The effect of a may be interpreted in terms of an adsorption time scale given by l/a; a smaller a describes slower adsorption. The overall effect of a on field-scale transport is similar to

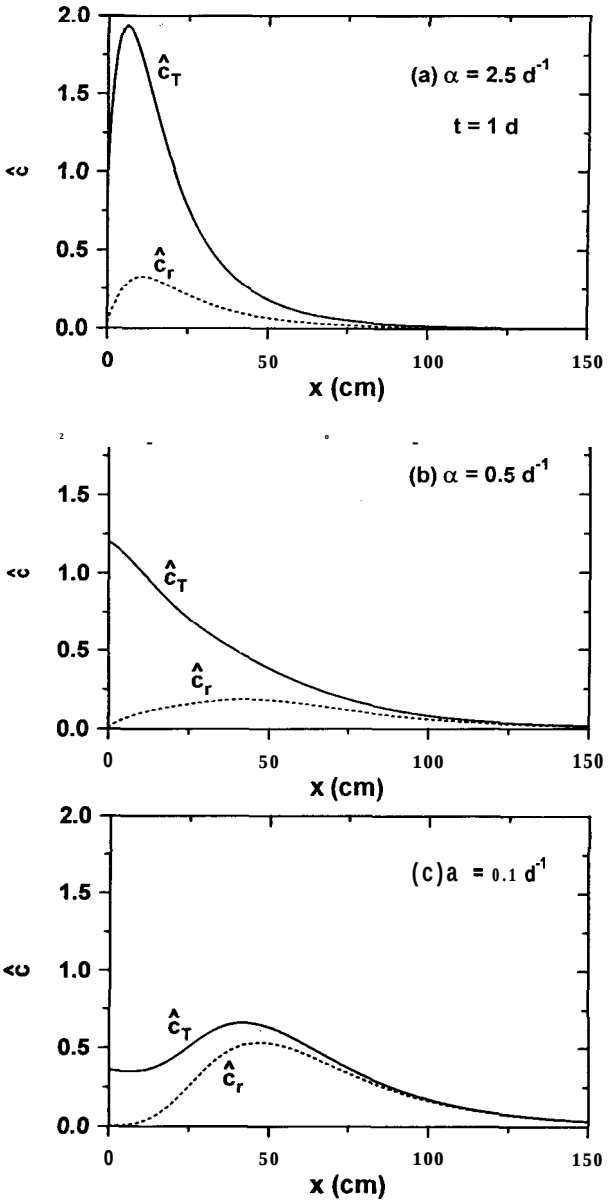

Pig. 8. Field-x-ate resident ($\hat{c}_r$) and total resident ($\hat{c}_T$) concentrations as a function of depth for three values of the nonequilibrium rate parameter, a, at time t = 1 d assuming a negative correlation between the distribution coefficient and the pore-water velocity, ρ_{vK_d} = — 1: (a) a = 2.5 d^{-1}, (b) a = 0.5 d^{-1}, and (c) a = 0.1 d^{-1}.

that for one-dimensional deterministic transport, i.e., the field-scale BTC becomes more skewed for-slower adsorption (van Genuchten and Cleary, 1979; Jury and Roth, 1990). Figure 8 shows calculated field-scale resident ($\hat{c}_r$) and total resident ($\hat{c}_T$) concentrations vs. depth at t = 1 d, assuming that v and K_d are stochastic parameters with ρ_{vK_d} = -1 for (a) a = 2.5 d^{-1}, (b) a = 0.5 d^{-1}, and (c) a = 0.1 d^{-1}. All other parameter values are the same as for Fig. 7. The difference between $\hat{c}_T$ and $\hat{c}_r$ reflects the amount of adsorbed solutes. As a decreases, some of the solutes will move downward faster because of delayed adsorption, while a relatively large fraction of the solutes will be adsorbed near the inlet for greater a.

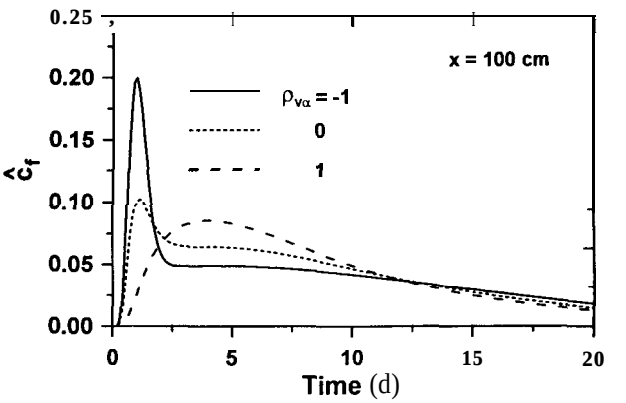

Fig. 9. Breakthrough curves for the field-scale flux-averaged concentration ($\hat{c}_f$) at x = 100 cm for three correlations between the pore-water velocity and the nonequilibrium parameter, $\rho_{v\alpha}$.

It is again possible to evaluate the effect of local-scale parameters on field-scale spreading at a certain depth, x, by comparing terms in the expressions for the variance, Var_t, given in Tables 2 and 3. The first term is related to nonequilibrium adsorption and the last term to velocity fluctuations. The ratio of the first to the last term is proportional to the ratio of the adsorption time scale, l/a, and inversely proportional to the convection time scale, $x/\langle v\rangle$. Solute spreading is primarily due to nonequilibrium adsorption when the adsorption time scale is larger than the convection time scale.

The prediction of field-scale concentrations becomes more complicated when the nonequilibrium rate coefficient, a, is a stochastic parameter. The effect of a random a on field-scale transport was investigated with the nonequilibrium CDE with $f(v,\alpha)$ assuming a deterministic K_d. Figure 9 shows $\hat{c}_f$, at x = 100 cm, vs. time for three values of $\rho_{v\alpha}$ with $\langle v\rangle$ = 50 cm d^{-1}, σ_v = 0.5, D = 20 $cm^2\,d^{-1}$, R = 5, <a> = 0.5 d^{-1}, and σ_α = 0.5. The BTC becomes more skewed for decreasing $\rho_{v\alpha}$. The variance is independent of $\rho_{v\alpha}$, as shown by the equation for Var_t in Table 2 for a stochastic v and a. The effect of $\rho_{v\alpha}$ is relatively similar to that of the nonequilibrium parameter, a, as demonstrated in Fig. 8. A negative correlation between v and a implies that adsorption is relatively slow in stream tubes with a high v and relatively fast for a small v. Figure 10 shows $\hat{c}_T$ and $\hat{c}_r$ profiles vs. depth at t = 1 d for $\rho_{v\alpha}$ = 1 and -1 with the same parameters as in Fig. 9. For a negative correlation, solutes in fast stream tubes move to relatively greater depths because of slower adsorption (Fig. 10b). Although field-scale transport is sensitive to $\rho_{v\alpha}$ as shown in Fig. 9 and 10, theoretical or experimental studies relating v and a are still lacking.

The peaking concentration will become smaller with distance, as observed in Fig. 9 for $\rho_{v\alpha}$ = — 1 at x = 100 cm. Figure 11 shows that early solute arrival and subsequent tailing due to the negative correlation between v and a may cause a bimodal breakthrough curve at greater depths. Destouni and Cvetkovic (1991) explained the same type of breakthrough curve with the physical nonequilibrium concept, which differentiates a mobile and an immobile liquid region. Because the deterministic

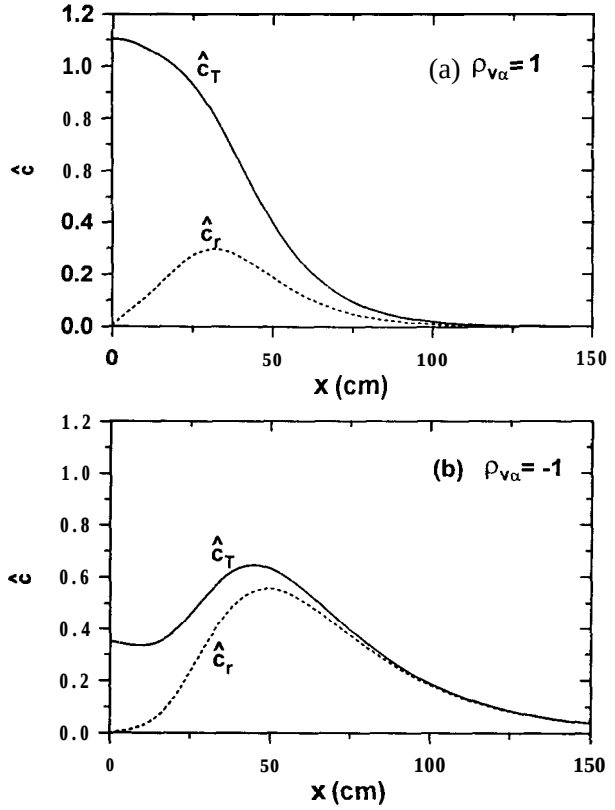

Fig. 10. Field-scale resident ($\hat{c}_r$) and total resident (ET) concentrations vs. depth for a perfect correlation between the pore-water velocity and the nonequilibrium rate parameter at t = 1 d: (a) $\rho_{v\alpha}$ = 1 and (b) $\rho_{v\alpha}$ = − 1.

transport equations for physical and chemical nonequilibrium are mathematically very similar, or sometimes identical such as for linear adsorption (e.g., Nkedi-Kizza et al., 1984), the two types of nonequilibrium should also give very similar breakthrough curves for stochastic transport. It appears more difficult to use the stream tube model for a physical than for a chemical nonequilibrium model for transport at the local scale. The formulation of a pdf in the former case is complicated due to the dependency of the pore-water velocity of each stream tube on the mobile water content. Although the pdf are more easily formulated for chemical nonequilibrium, the pdf for a may also be difficult to determine, especially when both v and K_d are stochastic.

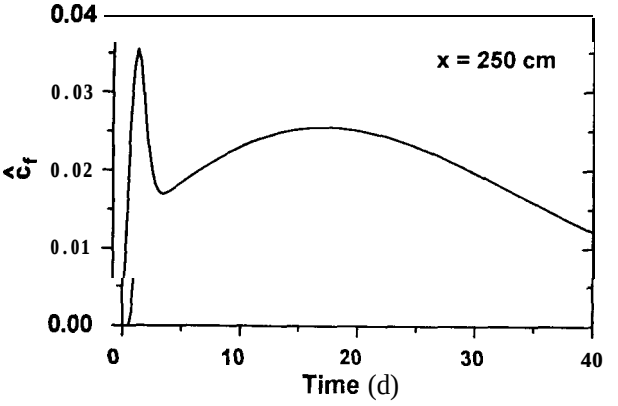

Fig. 11. Breakthrough curves for the geld-scale flux-averaged concentration ($\hat{c}_f$) at x = 250 cm for a perfect negative correlation between the pore-water velocity and the nonequilibrium parameter ($\rho_{v\alpha}$ = −1).

SUMMARY AND CONCLUSIONS

The downward movement of reactive and nonreactive chemicals across the field was described with the stochastic stream tube model with the CDE for local-scale equilibrium and nonequilibrium transport of reactive solutes. The effects of heterogeneous flow conditions at the field scale were demonstrated assuming pairs of random parameters for the local CDE. The pore-water velocity, v, was always considered to be a random parameter, while the additional random parameter was either the dispersion coefficient, D, the distribution coefficient for linear adsorption, K_d, or the first-order rate coefficient for adsorption, a. Field-scale mean concentrations were evaluated as ensemble averages of the analytical solutions for the CDE with a bivariate lognormal pdf for pairs of random transport parameters.

Three types of field-scale mean concentrations were defined for a stochastic velocity field based upon the local-scale concentration detection mode: (i) the ensemble average of the flux-averaged concentration, $\langle c_f \rangle$; (ii) the field-scale resident concentration, $\hat{c}_r$ ($= \langle c_r \rangle$); and (iii) the field-scale flux-averaged concentration, $\hat{c}_f$ ($= \langle vc_f \rangle / \langle v \rangle$). The latter reflects the solute flux across an entire field. The BTC for $\langle c_f \rangle$ and $\hat{c}_r$ showed similar distributions for most parameter combinations as long as the dispersivity is relatively small. The BTC for these ensemble averages contrasted with the BTC for $\hat{c}_f$, especially for a more heterogeneous flow field.

Expressions for first- and second-order time moments in terms of $\hat{c}_f$ were derived for three types of joint pdf, i.e., $f(v,D)$, $f(v,K_d)$, and $f(v,\alpha)$. The first moment, M_1, suggested that the variability in local parameters does not affect the mean breakthrough time. The variance, Var,, could be partitioned into terms for (i) nonequilibrium adsorption; (ii) local-scale dispersion, D; and (iii) differences in velocity between stream tubes. The effect of variability in the local-scale parameters on solute spreading was evaluated by comparing the magnitude of each term in the expression for Var_t. Among the three field-scale mean concentrations, both M_1 and Var_t were smallest for $\hat{c}_f$ and largest for $\hat{c}_r$.

As previously shown by Amoozegar-Fard et al. (1982) and Bresler and Dagan (1981), the effect of variability in **Don** mean solute distributions was minor as long as the Peclet number, $\langle v \rangle x / \langle D \rangle$, in terms of the observation scale, x, is relatively large. When the local-scale dispersivity ($\lambda = D/v$) is large, solute spreading due to local dispersion may still be considerable (especially for relative short travel distances). However, most previous studies of stochastic transport considered local-scale dispersion, D, to be negligible. We recommend to first estimate the Peclet number, $\langle v \rangle x / \langle D \rangle$, before deciding whether or not the effect of D can be neglected in the stream tube model (Fig. 4). An attractive simplification

is the use of a constant dispersivity across the field (i.e., $\rho_{vD} = 1$ and $\sigma_v = \sigma_D$).

For a stochastic distribution coefficient, K_d, solute spreading increased for negatively correlated v and K_d, even for small variations in K_d. For nonequilibrium adsorption, the field-scale BTC became more skewed for slower adsorption. This is in line with the observations for deterministic nonequilibrium transport. If the rate parameter, a, was stochastic, a negative correlation between v and a also enhanced the skewness of the solute distribution.

As long as the local-scale transport is linear, travel time moments can be used to characterize field-scale transport according to the stream tube model. Time moments presented in this paper characterized the effect of stochastic local-scale CDE parameters on field-scale solute distributions. In the second part of this study (Toride and Leij, 1996), the stream tube based upon the CDE is further investigated for various types of initial and boundary conditions that may be encountered in the field.

APPENDIX

Ensemble Averages for the Bivariate Lognormal Distribution

For the formulation of time moments of field-scale concentrations, we need to evaluate the ensemble average of $\langle \eta^n/v^m \rangle$. The average of this ratio is defined as

$$\left\langle \frac{\eta^n}{v^m} \right\rangle = \int_0^\infty \int_0^\infty \frac{\eta^n}{v^m} f(v,\eta)\, dv\eta \qquad [A1]$$

where $f(v,\eta)$ is a bivariate lognormal distribution given by Eq. [15]. Changing the integration variables to Y_v and Y_η as defined in Eq. [16] leads to

$$\left\langle \frac{\eta^n}{v^m} \right\rangle = \frac{\exp(n\mu_\eta - m\mu_v)}{2\pi\sqrt{1-\rho_{v\eta}^2}} \int_{-\infty}^{\infty}\int_{-\infty}^{\infty} \exp \times \left[-\frac{Y_v^2 - 2\rho_{v\eta}Y_\eta Y_v + Y_\eta^2}{2(1-\rho_{v\eta}^2)} - m\sigma_v Y_v + n\sigma_\eta Y_\eta \right] dY_v dY_\eta \qquad [A2]$$

Evaluation of these integrals is accomplished with identity (7.4.2) of Abramowitz and Stegun (1970), resulting in

$$\left\langle \frac{\eta^n}{v^m} \right\rangle = \exp\left(-m\mu_v + n\mu_\eta + \frac{m^2}{2}\sigma_v^2 - \rho_{v\eta} mn\sigma_v\sigma_\eta + \frac{n^2}{2}\sigma_\eta^2 \right) = \frac{\langle \eta \rangle^n}{\langle v \rangle^m} \exp \qquad [A3]$$

$$\left[\frac{m(m+1)}{2}\sigma_v^2 - \rho_{v\eta}\, mn\sigma_v\sigma_\eta + \frac{n(n-1)}{2}\sigma_\eta^2 \right]$$

REFERENCES

Abramowitz, M., and I.A. Stegun. 1970. Handbook of mathematical functions. Dover Publishing Co., New York.

Aitcheson, J., and J.A.C. Brown. 1963. The lognormal distribution. Cambridge University Press, London.

Amoozegar-Fard, A., D.R. Nielsen, and A.W. Warrick. 1982. Soil solute concentration distribution for spatially varying pore water velocities and apparent diffusion coefficients. Soil Sci. Soc. Am. J. 46:30-39.

Biggar, J.W., and D.R. Nielsen. 1976. Spatial variability of the leaching characteristics of a field soil. Water Resour. Res. 12:78-84.

Bosma, W.J.P., A. Bellin, S.E.A.T.M. van der Zee, and A. Rinaldo. 1993. Linear equilibrium adsorbing solute transport in physically and chemically heterogeneous porous formations 2. Numerical results. Water Resour. Res. 294031-4043.

Bresler, E., and G. Dagan. 1979. Solute dispersion in unsaturated heterogeneous soil at field scale: II. Applications. Soil Sci. Soc. Am. J. 43~467472.

Bresler, E., and G. Dagan. 1981. Convective and pore scale dispersive solute transport in unsaturated heterogeneous fields. Water Resour. Res. 17:1683-1693.

Cvetkovic, V.D., and A.M. Shapiro. 1990. Mass arrival of sorptive solute in heterogeneous porous media. Water Resour. Res. 26: 2057-2067.

Dagan, G. 1984. Solute transport in heterogeneous porous formation. J. Fluid Mech. 145151-177.

Dagan, G. 1993. The Bresler-Dagan model of flow and transport: Recent theoretical developments. p. 13-32. In D. Russo and G. Dagan (ed.) Water flow and solute transport in soils. Springer-Verlag, Berlin, Heidelberg.

Dagan, G., and E. Bresler. 1979. Solute dispersion in unsaturated heterogeneous soil at field scale: I. Theory. Soil Sci. Soc. Am. J. 4346-467.

Dagan, G., and V. Cvetkovic. 1993. Spatial moments of a kinetically sorbing solute plume in a heterogeneous aquifer. Water Resour. Res. 2940534061.

Destouni, G., and V.D. Cvetkovic. 1991. Field scale mass arrival of sorptive solute into the groundwater. Water Resour. Res. 27: 1315-1325.

Jury, W.A. 1982. Simulation of solute transport using a transfer function model. Water Resour. Res. 18:363-368.

Jury, W.A., and H. Flühler. 1992. Transport of chemicals through soils: Mechanism, model, and field applications. Adv. Agron. 47: 141-201.

Jury, W.A., W.R. Gardner, and W.H. Gardner. 1991. Soil physics. 5th ed. John Wiley & Sons, New York.

Jury, W.A., and K. Roth. 1990. Transfer functions and solute movement through soils: Theory and applications. Birkhäuser, Basel, Switzerland.

Jury, W.A., and D.R. Scotter. 1994. A unified approach to stochastic-convective transport problems. Soil Sci. Soc. Am. J. 58: 1327-1336.

Kabala, Z.J., and G. Sposito. 1991. A stochastic model of reactive solute transport with time-varying velocity in a heterogeneous aquifer. Water Resour. Res. 27:341-350.

Kreft, A., and A. Zuber. 1978. On the physical meaning of the dispersion equation and its solutions for different initial and boundary conditions. Chem. Eng. Sci. 33:1471-1480.

Leij, F.J., and J.H. Dane. 1991. Solute transport in a two-layer medium investigated with time moments. Soil Sci. Soc. Am. J. 55: 1529-1535.

Lindstrom, F.T., and M.N.L. Narasimhan. 1973. Mathematical theory of a kinetic model for dispersion of previously distributed chemicals in a sorbing porous medium. SIAM J. Appl. Math. 24: 496-510.

Nkedi-Kizza, P., J.W. Biggar, H.M. Selim, M. Th. van Genuchten, P.J. Wierenga, J.M. Davidson, and D.R. Nielsen. 1984. On the equivalence of two conceptual models for describing ion exchange during transport through an aggregated oxisol. Water Resour. Res. 20:1123-1130.

Robin, M.J.L., E.A. Sudicky, R.W. Gillham, and R.G. Kachanoski. 1991. Spatial variabilitv of Strontium distribution coefficients and their correlation with hydraulic conductivity in the Canadian forces base Borden aquifer. Water Resour. Res. 27:2619-2632.

Spiegel, M.R. 1992. Schaum's outline of theory and problems of

probabiiity and statistics, Schaum's outline series. McGraw-Hill, New York.
Sposito, G., and D.A. Barry. 1987. On the Dagan model of solute transport in groundwater: Foundational aspects. Water Resour. Res. 23:1867-1875.
Sudicky, E.A. 1986. A natural gradient experiment on solute transport in a sand aquifer: Spatial variability of hydraulic conductivity and its role in the dispersion process. Water Resour. Res. 22:2069-2082.
Toride, N., F.J. Leij, and M. Th. van Genuchten. 1993. Analytical solutions for nonequilibrium solute transport with first-order decay and zero-order production. Water Resour. Res. 29:2167-2182.
Toride, N., and F.J. Leij. 1996. Convective-dispersive stream tube model for held-scale solute transport: II. Examples and calibration. Soil Sci. Soc. Am. J. 60:352-361 (this issue).
Toride, N., F.J. Leij, and M. Th. van Genuchten. 1995. The CXTFIT code for estimating transport parameters from laboratory and field tracer experiments. U.S. Salinity Laboratory, Riverside, CA (in press).
Valocchi, A.J. 1985. Validity of the local equilibrium assumption for modeling sorbing solute transport through homogeneous soils. Water Resour. Res. 21:808-820.
van Genuchten, M. Th., and R.J. **Clcary. 1979. Movement of solutes** in soil: Computer-simulated and laboratory results. p. 349-386. In G.H. Bolt (ed.) Soil chemistry, B. Physical models. Elsevier, Amsterdam.
van der Zee, S.E.A.T.M., and W.H. van Riemsdijk. 1986. Transport of phosphate in a heterogeneous field. Transport Porous Media 1:339-359.
van der Zee, S.E.A.T.M., and W.H. van Riemsdijk. 1987. Transport of reactive solute in spatially variable soil systems. Water Resour. Res. 23:2059-2069.

#1431

Convective-Dispersive Stream Tube Model for Field-Scale Solute Transport: II. Examples and Calibration

Nobuo Toride and Feike J. Leij*

ABSTRACT

The use of the stream tube **model developed in the first part of this study is illustrated for several examples with a stochastic pore-water velocity, v, and distribution coefficient, K_d. The model allows quantification of the concentration variance in the horizontal plane to evaluate models for transport in heterogeneous fields. Increased vertical solute spreading due to stochastic local-scale parameters is accompanied by increased horizontal variations of the field-scale mean concentration. Solute application at the surface is modeled as a boundary value problem (BVP) and an initial value problem (IVP). The field-averaged concentration vs. depth exhibits more spreading for the BVP than the IVP since a variable solute mass is applied to each stream tube in the latter case. Flow is also modeled by a lognormal probability density function for the saturated conductivity, K_s, and the unit gradient assumption instead of v. The use of a random v instead of K_s is preferable for small variations in water content. Results of the stream tube model are compared with those of a one-dimensional macroscopic convection-dispersion equation (CDE) with effective parameters (i.e., depth-dependent constants). When these constants are determined from time moments of the field-scale flux-averaged concentration, $\hat{c}_f$, for the BVP, the stream tube model and the macroscopic CDE will give different results if the effective parameters are used to model other transport scenarios. Finally, the stream tube model was fitted to the concentrations obtained from a detailed numerical simulation of flow and transport in a (hypothetical) heterogeneous field. The (simple) stream tube model appears to provide a sensible description of the field-averaged concentration and variance.**

THE STREAM TUBE CONCEPT was presented in the first part of this study (Toride and Leij, 1996) for modeling solute transport in heterogeneous porous media. Transport in each stream tube was described with the CDE in which pairs of model parameters are considered realizations of a stochastic process that may be described with a bivariate lognormal pdf. The simplifications associated with the stream tube model may restrict its usefulness for many practical problems involving area-averaged transport. We will review the following aspects of applying the stream tube model to field-scale problems involving steady downward flow.

First, we will examine the variation of the solute concentration in the horizontal plane. Traditionally, spreading perpendicular to the direction of flow has not received as much attention as dispersion in the direction of flow. The horizontal solute distribution can be conveniently quantified with the stream tube model.

Second, an appropriate description of the initial and boundary conditions is needed before the stream tube model can be applied. Most previous studies of the stream tube model evaluated field-scale transport by solving the local-scale BVP with a Heaviside (continuous) or Dirac delta (instantaneous) type of solute input (e.g., Bresler and Dagan, 1979; Destouni and Cvetkovic, 1991). Solute application is described with a flux-mode boundary condition; the amount of mass in each stream tube is proportional to the local-scale v. Travel time moments were already derived for a Dirac delta input (Toride and Leij, 1996). Solute application at the surface of a field can also be described as an IVP. A resident mode concentration is used to quantify the solute application in this case, the solute is (initially) distributed uniformly across the field. Jury and Scotter (1994) discussed the difference between boundary and initial value problems for the stream tube model. We will further explore differences between the BVP and IVP for nonreactive and reactive solutes with a stochastic v.

Third, Dagan and Bresler (1979) investigated a stream tube type model assuming a lognormal pdf for the saturated hydraulic conductivity, K_s; V **was** calculated assuming a unit gradient in hydraulic head (gravitational flow).

N. Toride, Dep. of Agricultural Sciences, Saga Univ., Saga 840, Japan; and F.J. Leij, U.S. Salinity Lab., 450 West Big Spring Road, Riverside, CA 92507-4617. Contribution from the USDA-ARS Salinity Laboratory. Received 28 July 1994. *Corresponding author (fleij@ussl.ars.usda.gov).

Published in Soil Sci. Soc. Am. J. 60:352-361 (1996).

Abbreviations: BTC, breakthrough curve; BVP, boundary value problem; CDE, convection-dispersion equation; CV, coefficient of variance; IVP, initial value problem; pdf, probability density function.

Such an indirect approach of characterizing stochastic flow is often convenient since values for K_s are relatively easy to measure. This paper investigates the results of the stream tube model if either v or K_s is used as the basic stochastic parameter.

Fourth, solute transport in a heterogeneous field is sometimes described with a macroscopic, deterministic CDE with effective parameters. By adjusting transport parameters for different depths, a relatively simple mathematical model can, perhaps, be used to simulate transport in heterogeneous media. This approach is evaluated by comparing field-averaged solute profiles predicted by the macroscopic CDE and the stream tube model.

Finally, the utility of the (approximate) stream tube model can be assessed by comparing its predicted mean concentration and variance profiles with those obtained from a detailed numerical simulation of steady, unsaturated flow and transport in a hypothetical heterogeneous field.

STREAM TUBE MODEL

Let us assume that the pore-water velocity, v, and the distribution coefficient, K_d, are stochastic variables, which may be described with a bivariate lognonnal pdf. The local-scale concentration in each stream tube is obtained by solving the equilibrium or nonequilibrium CDE [Eq. [1] through [3] in Toride and Leij (1996)]. The field-scale resident concentration, $\hat{c}_r$, is equal to the ensemble average of the local-scale resident concentration, $\langle c_r \rangle$:

$$\hat{c}_r(x,t) = \langle c_r(x,t) \rangle = \int_0^\infty \int_0^\infty c_r(x,t;v,K_d) f(v,K_d) \mathrm{d}v \mathrm{d}K_d \qquad [1]$$

where $f(v,K_d)$ is the bivariate lognormal pdf with means $\langle v \rangle$ and $\langle K_d \rangle$, standard deviations σ_v and σ_{K_d}, and coefficient of correlation between ln v and $\ln K_d$, ρ_{vK_d} [Eq. [15] in Toride and Leij (1996)]. The field-scale total resident concentration is given by Eq. [24] in Toride and Leij (1996). The field-scale, flux-averaged concentration, $\hat{c}_f$, is defined as the ratio of the solute and water fluxes:

$$\hat{c}_f(x,t) = \frac{\langle v c_f \rangle}{\langle v \rangle} = \frac{1}{\langle v \rangle} \int_0^\infty \int_0^\infty v c_f(x,t;v,K_d) f(v,K_d) \mathrm{d}v \mathrm{d}K_d \qquad [2]$$

We described in Toride and Leij (1996) how the local-scale flux-averaged concentration, c_f, is related to c_r, and how Eq. [1] can also be used to define $\langle c_f \rangle$.

The dispersion coefficient, D, is also assumed to be stochastic and to be perfectly correlated with v. This is a reasonable assumption in view of the widely used relationship $D = \lambda v$, where λ is the dispersivity (cm). According to Eq. [22] in Toride and Leij (1996), we can write

$$D(v) = \left(\frac{v}{\langle v \rangle} \right)^{\sigma_D/\sigma_v} \langle D \rangle \exp\left(\frac{1}{2}\sigma_v \sigma_D - \frac{1}{2}\sigma_D^2 \right) \qquad [3]$$

where σ_v and σ_D are the standard deviations of ln v and ln D. All other local parameters, including the volumetric water content, θ, and the bulk density, ρ_b, are deterministic.

Fluctuations in the local-scale concentration at a particular depth, between stream tubes across the horizontal plane, can be characterized by the variance (Bresler and Dagan, 1981)

$$\mathrm{Var}[c(x,t)] = \int_0^\infty \int_0^\infty [c(x,t) - \langle c(x,t) \rangle]^2 f(v,K_d) \mathrm{d}v \mathrm{d}K_d = \langle c^2(x,t) \rangle - \langle c(x,t) \rangle^2 \qquad [4]$$

The variance for the field-scale flux-averaged concentration, $\hat{c}_f$, may be expressed as

$$\mathrm{Var}[v c_f(x,t)/\langle v \rangle] = \frac{1}{\langle v \rangle^2} \int_0^\infty \int_0^\infty [v c_f(x,t) - \langle v c_f(x,t) \rangle]^2 f(v,K_d) \mathrm{d}v \mathrm{d}K_d = \frac{1}{\langle v \rangle^2} [\langle v^2 c_f^2(x,t) \rangle - \langle v c_f(x,t) \rangle^2] \qquad [5]$$

The solutions for the BVP and IVP in terms of the field-scale stream tube model follow directly from the local-scale solution for each tube, with boundary and initial conditions

$$c_r(x,0) = c_i(x), \qquad s(x,0) = K_d c_i(x) \qquad [6a,b]$$

$$v c_r(0,t) - D \frac{\partial c_r(0,t)}{\partial x} = v g(t) \qquad [7]$$

$$\frac{\partial c_r}{\partial x}(\infty,t) = 0 \qquad [8]$$

where c_i and g are the initial and input concentrations (g cm^{-3}), respectively, and s is the adsorbed concentration (g g^{-1}). Solutions of the equilibrium and nonequilibrium CDE are available for several initial and boundary conditions (e.g., van Genuchten and Alves, 1982; Toride et al., 1993). Field-scale concentrations and variances were evaluated by substituting the appropriate analytical solution for the local-scale concentration and the joint pdf into Eq. [1], [2], [4], or [5], as discussed in Toride and Leij (1996). Details on the analytical solutions for the CDE and the numerical evaluation of field-scale concentrations are given by Toride et al. (1995).

RESULTS AND DISCUSSION

Conceritration Variation in the Horizontal Plane

Figure 1 shows the mean, $\hat{c}_r = \langle c_r \rangle$, and variance according to Eq. [4] as a function of depth for three values of σ_v at $t = 3$ d after a single pulse application of a nonreactive solute (R = 1) for 2 d with $\langle v \rangle = 20$ cm d^{-1}, $D = 20$ cm^2 d^{-1}, and $\sigma_D = 0$. All concentrations are assumed to be normalized.

More solute spreading occurs in the &-profile when σ_v increases (Fig. la). Figure lb shows that the variation in the local-scale c_r also increases with σ_v, indicating that a more heterogeneous solute distribution will occur in the horizontal plane. Because flow and transport become more heterogeneous as σ_v increases, more observations are needed to reliably estimate field-scale mean values when σ_v equals 0.5 instead of 0.1. The variance profiles have a double peak with a relative minimum around x = 30 cm (Fig. lb) where the highest concentration occurs (Fig. la). A similar bimodal behavior of the variance

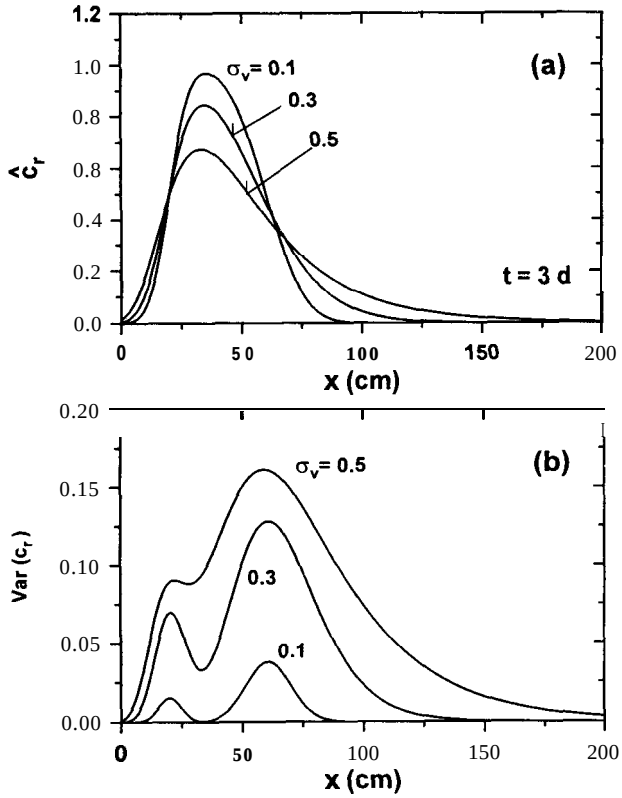

Fig. 1. The effect of the variability in the pore-water velocity, v, on (a) the field-scale resident concentration ($\hat{c}_r$) profile, and (b) the distribution of the variance for c_r in the horizontal plane with three values of the standard deviation, σ_v, at time, t = 3 d for a nonreactive solute as a result of a pulse input for 2 d to an iniitally solute-free soil (x = depth).

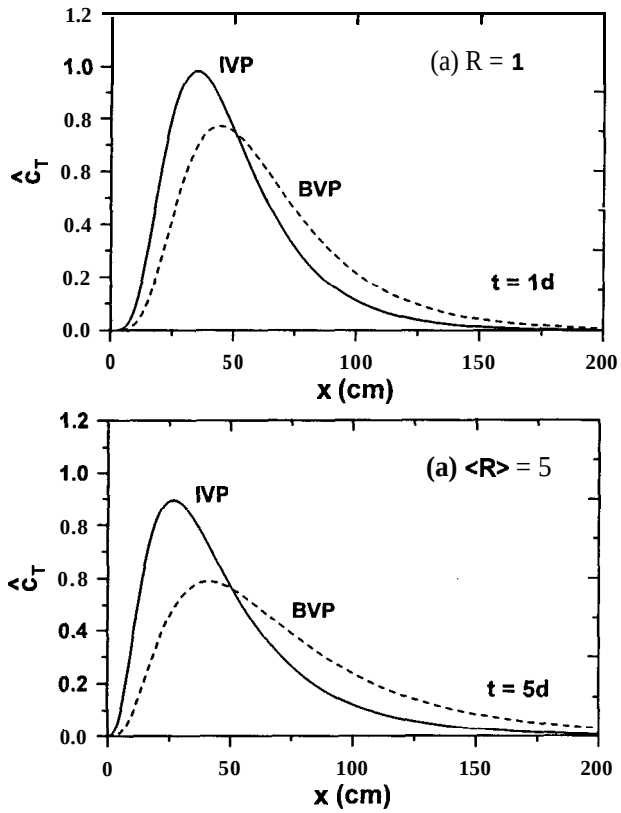

Fig. 2. Field-scale total resident concentrations ($\hat{c}_T$) vs. depth, x, for a Dirac delta application based upon the boundary value problem (BVP) and initial value problem (IVP) formulation for (a) a nonreactive solute at time, t = 1 d and (b) a reactive solute (<R> = 5) at t = 5 d.

was observed by Burr et al. (1994) for a numerical simulation of transport in three dimensional heterogeneous media. The variance also depends on the duration of the solute application. Continued solute injection will counteract the variance caused by random solute transport and the variance will decrease.

Boundary and Initial Value Problems

Consider solute application to the surface of an initially solute-free soil. The initial and boundary conditions for this case are given by Eq. [6] through [8] with $c_i = 0$. For a BVP involving instantaneous solute application, g(t) in Eq. [7] is given as

$$g_r(t) = \frac{m_B}{v}\delta(t) \qquad [9]$$

where $\sigma(t)$ is the Dirac delta function (d^{-1}), and m_B is the amount of mass added to a unit area of the liquid phase in the soil (g cm^{-2}). The amount of mass added to a unit area of soil is given by θm_B. Note that the input mass, m_B, is proportional to v due to the third-type inlet condition (Eq. [7]). The mass applied to an individual stream tube, m_B equals $v<m_B>/<v>$.

A very similar transport scenario can be described as an IVP. Consider a solute that is initially distributed uniformly across the soil surface; solute free water is subsequently applied to the surface. The initial distribution (a solute spike at x = 0) is given by

$$c_i(x) = \frac{m_I}{\theta}\delta(x) \qquad [10]$$

where $\delta(x)$ is a Dirac delta function (cm-'), m_I is the amount of mass present in the solution phase per unit soil area (g cm^{-2}). The IVP according to Eq. [10] implies that the same amount of solute, m_I, is present in all stream tubes regardless of v. Note that solutions of the BVP and the IVP are identical for the deterministic equilibrium CDE when $m_B = m_I/R\theta$ (Jury and Roth, 1990, p. 61), whereas solutions for the nonequilibrium CDE are slightly different for the BVP and IVP because of the kinetic desorption process (Toride et al., 1993).

Figure 2a shows the total resident combination, $\hat{c}_T$, as a function of depth at t = 1 d according to the solution of the BVP (Eq. [9]) and the IVP (Eq. [10]) for a nonreactive solute with <v> = 50 cm d^{-1}, <D> = 20 $cm^2 d^{-1}$, and $\sigma_v = \sigma_D = 0.5$. Note that the soil contains the same amount of solute (<m_B> = m_I/θ) for the BVP and the IVP. More solute remains near the surface for the IVP, while somewhat faster downward movement occurs for the BVP since a larger fraction of solutes resides in stream tubes with a higher velocity as a result of the velocity dependent injection mode (Jury and Scotter, 1994). If m_B is constant for all stream tubes, the $\hat{c}_r$ profile

is identical for the BVP and the IVP. We also note that for the equilibrium CDE with a constant K_d, the ensemble average of the flux-averaged concentration, $\langle c_f \rangle$, for the BVP is identical to the field-scale flux-averaged concentration, $\hat{c}_f$, for the IVP [see Fig. 5 in Toride and Leij (1995)].

The differences between the BVP and IVP increase if the BVP and the IVP are solved for a reactive solute. Figure 2b shows $\hat{c}_T$ profiles at t = 5 d for a reactive solute, assuming that $\langle m_B \rangle = m_l/\langle R \rangle\theta$ with $\langle R \rangle$ = 5, ρ_b/θ = 4 g cm^{-3}, $\langle K_d \rangle$ = 1 g^{-1} cm^3, σ_{K_d} = 0.2, and $\rho_{vK_d} = -1$. The same flow parameters were used as for Fig. 2a. The solution of the IVP predicts a slightly different solute amount in each stream tube since K_d is stochastic, and a greater solute fraction remains near the surface after 5 d than for the nonreactive solute after 1 d.

Because the stream tube model does not permit mixing between tubes, the solutions based upon the local-scale BVP and IVP constitute two limiting cases. Redistribution between stream tubes is likely to establish an intermediate scenario where the mass in each stream tube is not constant, as assumed in the IVP, but the differences between tubes are not as large as for the BVP because of horizontal mixing. In reality, some horizontal mixing could also occur at the surface. The mathematical description of the solute application has to be selected based upon the horizontal mass distribution if the stream tube model is used to describe field-scale transport.

Leaching of Reactive Solute

Relatively little attention has been paid to the use of the stream tube model in conjunction with the IVP. We will discuss two typical scenarios for leaching of reactive solutes with equilibrium and nonequilibrium adsorption with the analytical solutions of the CDE for a stepwise initial distribution (Toride et al., 1993).

Figure 3 presents the mean, $\hat{c}_r$ (= $\langle c_r \rangle$), and the variance of c_r as a function of depth with three values of ρ_{vK_d} at t = 3 d for the application of solute-free water to a soil with a stepwise initial distribution as shown in Fig. 3a. The following values were used: $\langle v \rangle$ = 50 cm d^{-1}, $\langle D \rangle$ = 20 cm^2 d^{-1}, $\sigma_v = \sigma_D$ = 0.5, $\langle R \rangle$ = 5, ρ_b/θ = 4 g cm^{-3}, $\langle K_d \rangle$ = 1 g^{-1} cm^3, and σ_{K_d} = 0.2. In this example, it is assumed that solutes in the liquid and adsorbed phases are always at equilibrium. Although a negative correlation between v and K_d enhances solute spreading in a similar manner as for the BVP [Fig. 7 in Toride and Leij (1996)], the spreading is less than observed for the BVP (Fig. 2). Figure 3b illustrates an increase in the variance for $\rho_{vK_d} = -1$, while a similar bimodal behavior occurs as for the BVP (Fig. lb).

Figure 4 presents field-scale resident ($\hat{c}_r$) and total resident ($\hat{c}_T$) concentration profiles at t = 3 d for the same problem but now with nonequilibrium adsorption [Eq. [2] in Toride and Leij (1996)]. Three values are used for the rate coefficient, a, including equilibrium adsorption ($a \rightarrow \infty$). The field-scale total resident concentration consists of solutes in the liquid and adsorbed phases ($\hat{c}_T = \hat{c}_r + \rho_b \langle s \rangle/\theta$). Note that the $\hat{c}_r$ profile

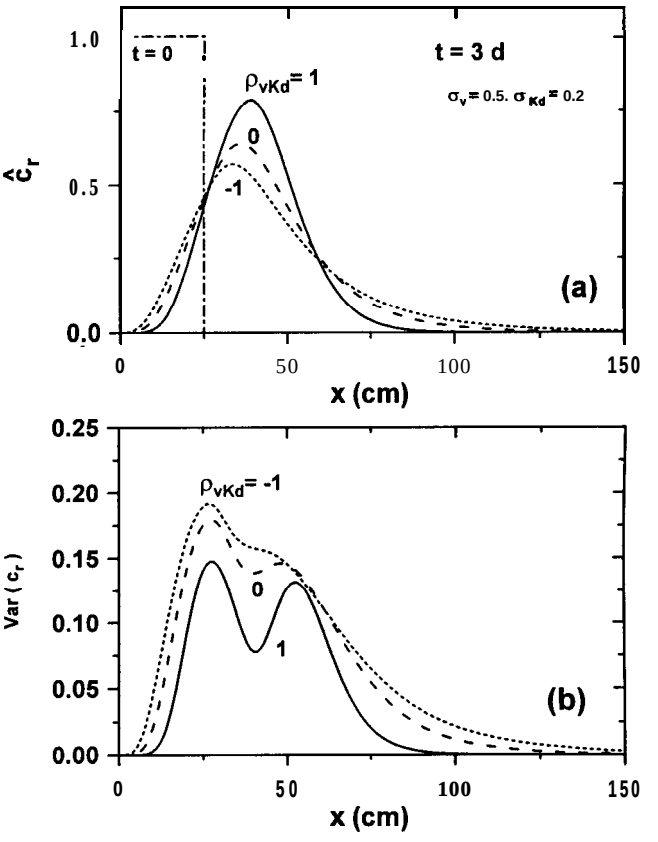

Fig. 3. The effect of the correlation between pore-water velocity, v, and distribution coeliicient, K_d at time, t = 3 d, for leaching of a reactive solute by applying solute-free water to a soil with a stepwise initial distribution: (a) the field-scale resident concentrations ($\hat{c}_r$), and (b) the variance for c_r (Var = variance; x = depth).

for the equilibrium case (Fig. 4c) is identical to the dotted line for $\rho_{vK_d} = -1$ shown in Fig. 3a. For nonequilibrium adsorption, the &-profile still resembles the initial distribution at t = 3 d because of the slow desorption rate. For equilibrium adsorption, 80% of the solute at this time has already leached below x = 25 cm, whereas for the nonequilibrium cases with a = 0.1 and 0.5 d^{-1}, 66 and 42% of the solute remains in the upper 25 cm of the profile, respectively. Once desorption takes place, the leaching process will proceed faster because of the slower adsorption of solutes from the liquid phase in case of nonequilibrium. Knowledge of the adsorption time scale is important to assess contamination risks.

Lognormal Probability Density Function for Saturated Hydraulic Conductivity

Dagan and Bresler (1979), Bresler and Dagan (1979), and Bresler and Dagan (198 1) described heterogeneous unsaturated flow with the stream tube model assuming a lognormal pdf for the saturated hydraulic conductivity, K_s. We will evaluate the flow field according to their assumptions and compare it with the lognormal distribution for the pore-water velocity, v, used in this study. The lognormal pdf for K_s may be written as

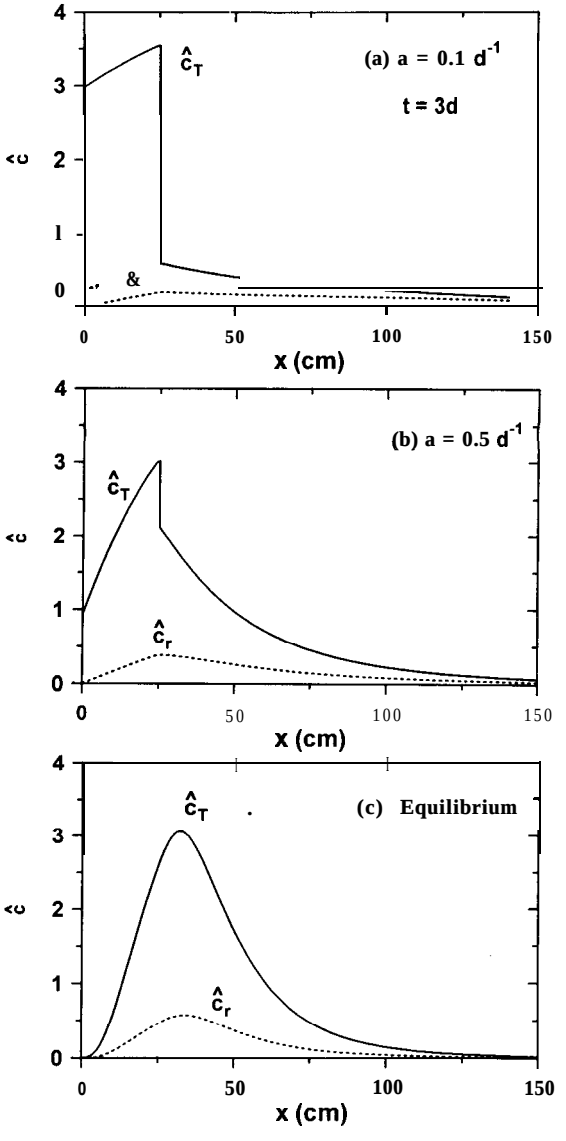

Fig. 4. The effect of nonequilibrium rate parameter *(a)* on the field-scale total ($\hat{c}_T$) and resident ($\hat{c}_r$) concentration profiles at t = 3 d as the result of applying solute-free water to a soil with a stepwise initial distribution: (a) a = 0.1 d^{-1}, (b) α = 0.5 d^{-1}, and (c) equilibrium ($\alpha \to \infty$) (x = depth).

$$f(K_s) = \frac{1}{\sqrt{2\pi}\sigma_{K_s}K_s}\exp\left(-\frac{[\ln(K_s) - \mu_{K_s}]^2}{2\sigma_{K_s}^2}\right) \quad [11]$$

where μ_{K_s} and σ_{K_s} are the mean and standard deviation of In K_s, respectively, and where the ensemble average is defined similar to Eq. [18] in Toride and Leij (1996), i.e., $\langle K_s \rangle = \exp(\mu_{K_s} + \sigma_{K_s}^2/2)$. The local-scale pore-water velocity, v, in each stream tube was obtained by the unsaturated hydraulic conductivity according to Brooks and Corey (1964):

$$K(\theta) = K_s\left(\frac{\theta - \theta_r}{\theta_s - \theta_r}\right)^{1/\beta} \quad [12]$$

where β is an empirical constant, and θ_r and θ_s are the residual and saturated water contents, respectively. Steady water flow was assumed to occur as a result of a constant surface recharge rate, r, with respect to time. If $r < K_s$, the soil is unsaturated and v is obtained by assuming gravitational flow at a uniform water content:

$$v = \frac{K(\theta)}{\theta} = \frac{r}{\theta} \quad [13]$$

Ponding occurs if $r > K_s$ in which case the soil is saturated:

$$\theta = \theta_s, \qquad v = \frac{K_s}{\theta_s} \quad (r \geq K_s) \qquad [14a,b]$$

If we assume that water can indeed be applied uniformly, which is unlikely because lateral water flow will occur at the surface while ponding results in an increased r, and if $\theta_r = 0$, the water content and the pore-water velocity can be given as a function of K_s (Eq. [12] and [13]):

$$\theta = \theta_s\left(\frac{r}{K_s}\right)^{\beta}, \qquad v = \frac{r^{1-\beta}K_s^{\beta}}{\theta_s} \quad (r < K_s) \quad [15a,b]$$

Figure 5a shows a lognormal pdf for K_s when $\langle K_s \rangle$ = 20 cm d^{-1} and σ_{K_s} = I; the CV is 131% [Eq. [19] in Toride and Leij (1996)]. Figure 5b and 5c present θ and v according to Eq. [14] and [15] as a function of K_s for four recharge rates, r, assuming θ_s = 0.4 and 1/β = 7.2 (Dagan and Bresler, 1979). Because of the unit-gradient assumption, the Darcy water flux, $v\theta$, equals r for unsaturated flow; only changes in water content, θ, will affect v in this case. Hence. v increases only minimally for $r < K_s$, as shown in the right side of Fig. 5c, whereas v increases linearly with K_s for saturated conditions (Eq. [14b]). The fraction of stream tubes with saturated flow, which depends for a given r on the pdf for K_s shown in Fig. 5a, is equal to the probability that $K_s \leq r$. In our case, there is a 19% probability that $K_s \leq r$ if r = 5 cm d^{-1}, 69% for r = 20 cm d^{-1}, 92% for r = 50 cm d^{-1}, and 98% for r = 100 cm d^{-1}. If r is much greater than $\langle K_s \rangle$, for example r = 100 cm d^{-1}, ponding occurs almost everywhere. On the other hand, if r is much less than $\langle K_s \rangle$, such as r = 5 cm d^{-1}, flow is mainly unsaturated with an almost uniform v across the field due to the unit gradient assumption.

Since K_s is described with a lognormal distribution, the corresponding pdf for the pore-water velocity, *f(v),* given by Eq. [14b] and [15b], is also described with a lognormal distribution containing the following parameters (Aitcheson and Brown, 1963, p. 11; Jury and Roth, 1990, p. 65): $\mu_v = \ln(1/\theta_s) + \mu_{K_s}$ and $\sigma_v = \sigma_{K_d}$ for $0 < v < r/\theta_s$; and $\mu_v = \ln(r^{\beta-1}/\theta_s) + \beta\mu_{K_s}$ and $\sigma_v = \beta\sigma_{K_d}$ for $v \geq r/\theta_s$ (Eq. [15b]). Figure 6 presents *f(v)* as a result of four recharge rates with the same conditions as for Fig. 5. The pdf is discontinuous at $v = r/\theta_s$ because of the different assumptions for saturated (Eq. [14]) and unsaturated (Eq. [15]) flow. For the admittedly high value of r = 100 cm d^{-1} (Fig. 6b), the resulting *f(v)* is almost identical to the lognormal *f(v),* while for r = 5 cm d^{-1} (Fig. 6a), *f(v)* based upon Eq. [15b] has a sharp peak, indicating almost uniform flow. The pdf for $r \approx \langle K_s \rangle$ = 20 cm d^{-1}, however, has a double peak because of the simultaneous occurrence of both

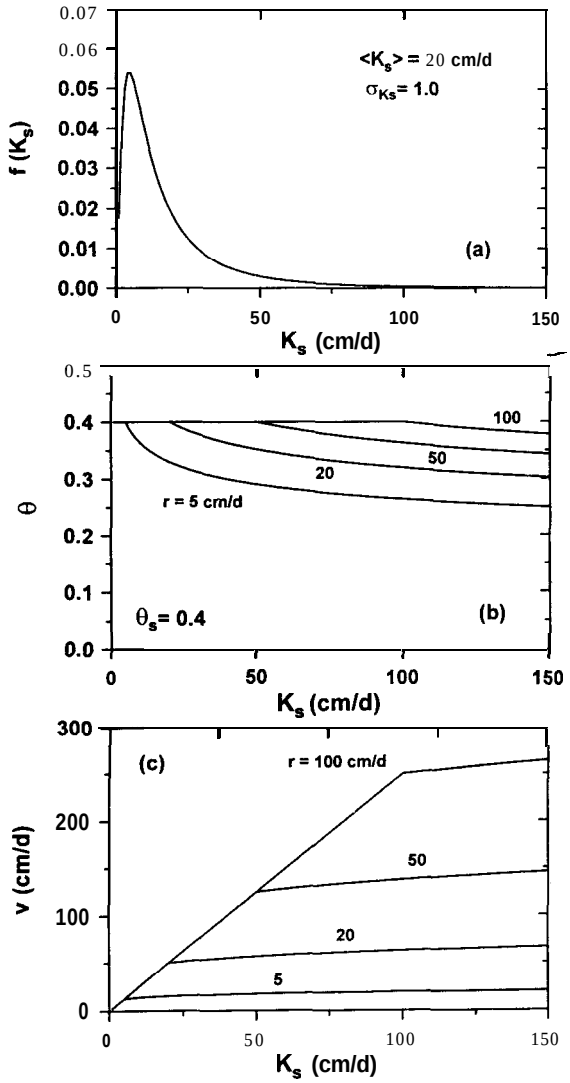

Fig. 5. Gravitational flow for the stream tube model assuming a lognormal probability density function (pdf) for the saturated hydraulic conductivity, K_s, as a result of four recharge rates, r: (a) lognormal pdf for K_s with $\langle K_s \rangle$ = 20 cm d^{-1}, and σ_{K_s} = 1, (b) water content, θ, vs. K_s, and (c) pore-water velocity, v, vs. K_s.

heterogeneous saturated flow and homogeneous unsaturated flow.

Excess water as a result of $r > K_s$ is not allowed to move to other stream tubes with a higher K_s. The example of ponding is therefore somewhat unrealistic. The uniformity of unsaturated flow in stream tubes with a high K_s can be attributed to a lack of water supply form tubes with a lower K_s. In reality, preferential flow may occur in a fracture whose conductivity is higher than that in the surrounding area because excess water will move toward such a fracture. Figures 5 and 6 demonstrate that the lognormal pdf for K_s in conjunction with the unit gradient assumption to predict the unsaturated velocity may be unrealistic. On the other hand, application of the lognormal pdf for v, as also used in Toride and Leij (1996), assumes a constant θ across the field. For unsaturated flow, however, both θ and v are stochastic. As a first approximation, the use of a constant θ and a lognormal pdf for v is probably appropriate for the stream

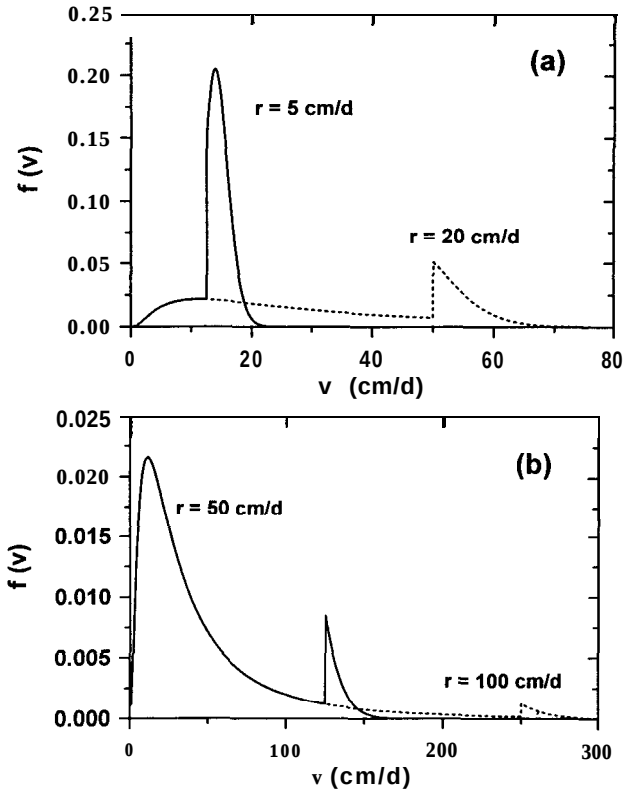

Fig. 6. The probability density function (pdf) for the pore-water velocity, v, as a result of gravitational flow based upon the lognormal pdf for K_s with the recharge rates: (a) r = 5 and 20 cm d^{-1}, and (b) r = 50 and 100 cm d^{-1}.

tube model as long as the CV is much lower for θ than for v.

Macroscopic Convection-Dispersion Equation

Solute transport in a heterogeneous field is sometimes described with a one-dimensional macroscopic CDE with effective parameters (Sposito et al., 1986). Although mathematically and physically incorrect, this approach is still being used since it simplifies the simulation of transport in heterogeneous media. The dependency of effective parameters, such as the dispersion coefficient, on the solute travel time or travel distance is often used to characterize the heterogeneous nature of transport (Khan and Jury, 1990; Porro et al., 1993). The macroscopic CDE will be used here to model transport in accordance with the stream tube model. The one-dimensional macroscopic CDE for a field-scale resident concentration, $\hat{c}_r$, may be described as where the superscript eff refers to an effective parameter, which is assumed constant when solving

$$R^{\text{eff}}\frac{\partial \hat{c}_r}{\partial t} = D^{\text{eff}}\frac{\partial^2 \hat{c}_r}{\partial x^2} - v^{\text{eff}}\frac{\partial \hat{c}_r}{\partial x} \qquad [16]$$

the transport problem for a particular depth. The boundary and initial conditions for $\hat{c}_r$ are identical to those for the conventional CDE (Eq. [6] through [8]), except that effective parameters are used. The initial adsorbed concentration for a stochastic distribution coefficient K_d,

may be given by 4(x, 0) = $\langle K_d \rangle c_i(x)$. We can obtain $\hat{c}_f$ from $\hat{c}_r$ with

$$\hat{c}_f = \hat{c}_r - \frac{D^{eff}}{v^{eff}} \frac{\partial \hat{c}_r}{\partial x} \quad [17]$$

Values for the effective parameters are obtained from moments for the stream tube model; we will use the first two time moments for $\hat{c}_f$ as a result of a Dirac input. When the position, x, is equal to the travel distance, Ax, the first normalized time moment, M_1, for the macroscopic CDE is given by [Table 1 in Toride and Leij (1996)]

$$M_1(\Delta x;\hat{c}_f) = \frac{R^{eff}\Delta x}{v^{eff}} \quad [18]$$

while the central second moment or variance, Var_t, is written as

$$\mathrm{Var}_t(\Delta x;\hat{c}_f) = \frac{2D^{eff}(R^{eff})^2\Delta x}{(v^{eff})^3} \quad [19]$$

Effective parameters can be obtained if M_1 and Var_t are known. This example involves $\hat{c}_f$ modeled with a stochastic v and K_d. Substitution of the expression for $M_1(\Delta x;\hat{c}_f)$ in Table 2 of Toride and Leij (1996) into Eq. [18] leads to

$$\frac{v^{eff}}{R^{eff}} = \frac{\langle v \rangle}{\langle R \rangle} \quad [20]$$

where $\langle R \rangle$ is given by $1 + \rho_b \langle K_d \rangle/\theta$. For a nonreactive tracer ($\langle R \rangle = R^{eff} = 1$), v^{eff} is equal to the ensemble average $\langle v \rangle$. If $v^{eff} = \langle v \rangle$, it follows that for a reactive solute $R^{eff} = \langle R \rangle$. An expression for the effective dispersion coefficient, D^{eff}, was obtained by inserting the equation for $\mathrm{Var}_t(\Delta x;\hat{c}_f)$ in Table 2 of Toride and Leij (1996) into Eq. [19] while assuming that $v^{eff} = \langle v \rangle$ and $R^{eff} = \langle R \rangle$. The result is

$$D^{eff}(\Delta x;\hat{c}_f) =$$

$$\frac{\rho_b\langle K_d\rangle}{\alpha\theta\langle R\rangle^2} + \frac{D}{\langle R\rangle^2}\exp(3\sigma_v^2)\left[1 + \frac{2\rho_b\langle K_d\rangle}{\theta}\exp(-2\rho_{vK_d}\sigma_v\sigma_{K_d}) + \frac{\rho_b^2\langle K_d\rangle^2}{\theta^2}\exp(-4\rho_{vK_d}\sigma_v\sigma_{K_d} + \sigma_{K_d}^2)\right] + \frac{\langle v\rangle\Delta x}{2\langle R\rangle^2}$$

$$\left\{\exp(\sigma_v^2) - 1 + \frac{2\rho_b\langle K_d\rangle}{\theta}\cdot[\exp(\sigma_v^2 - \rho_{vK_d}\sigma_v\sigma_{K_d}) - 1] + \frac{\rho_b^2\langle K_d\rangle^2}{\theta^2}[\exp(\sigma_v^2 - 2\rho_{vK_d}\sigma_v\sigma_{K_d} + \sigma_{K_d}^2) - 1]\right\} \quad [21]$$

This expression can be further simplified for equilibrium adsorption or for nonreactive solute transport. Notice that D^{eff} increases linearly with the travel distance, Ax, because the third term in Eq. [21] is proportional to Ax.

Figure 7 compares the use of the stream tube model with the corresponding macroscopic CDE to predict BTC, at two positions, in terms of $\hat{c}_f$ as a result of a l-d application of a nonreactive (Fig. 7a) and a reactive (Fig. 7b) solute to an initially solute-free field. The stream tube parameters are $\langle v \rangle$ = 20 cm d^{-1}, σ_v = 0.5, and D = 10 cm^2 d^{-1} while the parameters for the macroscopic CDE are v^{eff} = 20 cm d^{-1}, R^{eff} = 1, D^{eff} = 305 cm^2 d^{-1} for x = 100 cm and D^{eff} = 589 cm^2 d^{-1} for x = 200 cm. Additional parameters for a reactive solute undergoing equilibrium adsorption ***(a-m)*** are $\langle K_d \rangle$ = 1 cm^3 g^{-1}, σ_{K_d} = 0.2, ρ_b/θ = 4 g cm^{-3}, $\langle R \rangle$ = 5, and $\rho_{vK_d} = -1$ for the stream tube model, and R^{eff} = 5, D^{eff} = 580 cm^2 d^{-1} for x = 100 cm, and D^{eff} = 1130 cm^2 d^{-1} for x = 200 cm if the macroscopic CDE is used. The BTC for the stream tube model and the macroscopic CDE agree well for both the nonreactive and reactive solute, although only the first two moments of $\hat{c}_f$ were used.

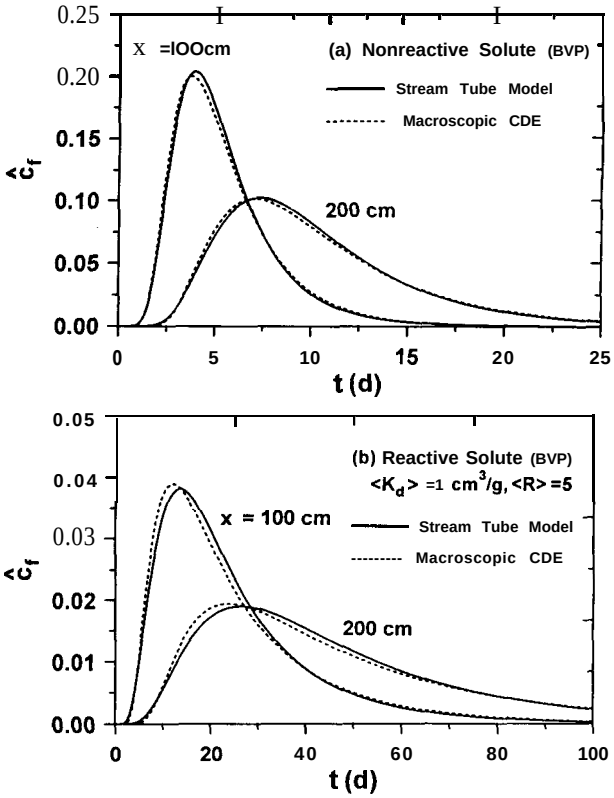

Fig. 7. Comparison of the stream tube model with the macroscopic convection-dispersion equation (CDE) for predicting field-scale breakthrough curves in terms of flux-averaged concentration, $\hat{c}_f$, at x = 100 and 200 cm as a result of a l-d solute input to an initially solute-free field for (a) a nonreactive solute, and (b) a reactive solute (BVP = boundary value problem; x = depth).

There is no guarantee, however, that the macroscopic CDE with the above parameters can be used for other transport problems (e.g., the solution of the IVP, prediction of field-scale resident concentrations). Different time moments should be used in such cases, and the effective parameters will change accordingly. In reality, effective parameters are usually determined from limited sets of concentration data. In the following, we will illustrate how well the macroscopic CDE, with effective parameters determined from the BTC in terms of $\hat{c}_f$ for a BVP, predicts field-scale transport for other conditions.

Figure 8 presents BTC for $\hat{c}_f$ at x = 100 and 200 cm as the result of a stepwise initial distribution for a nonreactive solute (c_i = 1, 0 < x < 25 cm; c_i = 0, x >

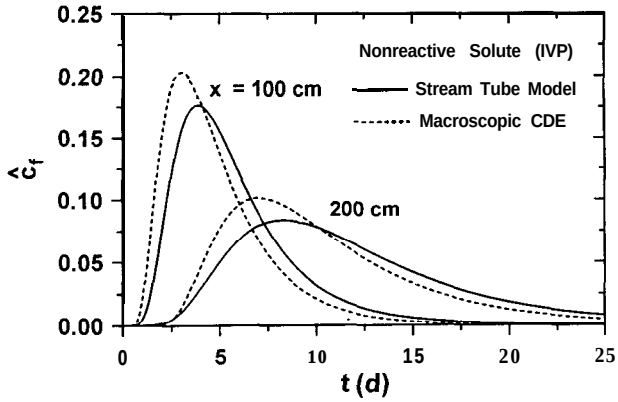

Fig. 8. Comparison of the stream tube model with the macroscopic convection-dispersion equation (CDE), with effective parameters based on the boundary value problem, for predicting field-scale breakthrough curves in terms of flux-averaged $\hat{c}_f$, at x = 100 and 200 cm as a result of applying solute-free water to a soil having a stepwise initial distribution of a nonreactive solute (c_i = 1, 0 < x < 25 cm; c_i = 0, x > 25 cm) (IVP = initial value problem; x = depth).

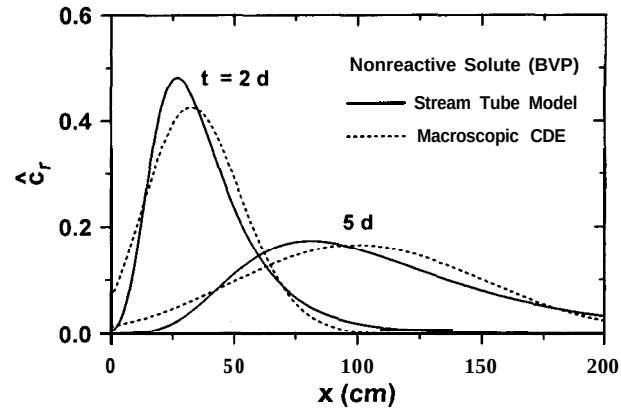

Fig. 9. Comparison of the stream tube model with the macroscopic convection-dispersion equation (CDE), with effective parameters based on the breakthrough curves in terms of flux-averaged concentration, $\hat{c}_f$, for predicting &-profiles at t = 2 and 5 d as a result of a l-d application of a nonreactive solute to an initially solute-free field (BVP = boundary value problem; x = depth).

25 cm). The stream tube model and the macroscopic CDE use the same parameters as for Fig. 7a. The effective dispersion coefficient, D^{eff}, described with Eq. [21] is a function of the travel distance from the surface, Ax. Note that the travel distance for the BVP is not exactly the same as that for the IVP. The BTC in Fig. 8 displays a higher peak concentration and earlier breakthrough for the macroscopic CDE than for the stream tube model. At x = 200 cm, the BVP (Fig. 7a) and IVP (Fig. 8) give almost identical results for the macroscopic CDE, whereas the BTC are different for the BVP and the IVP if the stream tube model is used. As was pointed out in the discussion of Fig. 2, the stream tube model assumes that a large fraction of the solute resides in stream tubes with a higher velocity for the BVP, while all stream tubes have the same solute mass for the IVP. On the other hand, the one-dimensional macroscopic CDE assumes a uniform solute distribution in the horizontal plane for both the BVP and IVP.

If we replace Ax in Eq. [21] by $<v>\Delta t$, where At is the travel time, D^{eff} at $t = \Delta t$ may be given by Eq. [21]. Figure 9 shows the field-scale resident concentration, $\hat{c}_r$, vs. depth, at t = 2 and 5 d as result of a l-d application of a nonreactive solute. The same parameter values are used in the stream tube model as in Fig. 7a. We also assumed that Eq. [20] and [21], which are based on time moments for the field-scale flux-averaged concentration, $\hat{c}_f$, can be used for estimating the field-scale resident concentration, $\hat{c}_r$. The effective parameters for the macroscopic CDE are now $v^{eff} = <v> = 20$ cm d^{-1}, $R^{eff} = 1$, and $D^{eff} = 134$ $cm^2\,d^{-1}$ for t = 2 d and $D^{eff} = 305$ $cm^2\,d^{-1}$ for t = 4 d. The agreement between the stream tube model and the macroscopic CDE for the &-profile in Fig. 9 is poor compared with the BTC for $\hat{c}_f$ in Fig. 7a. The concentration near the surface decreases rapidly with time for the stream tube model, whereas the macroscopic CDE predicts a higher concentration near the surface at both times because of a relatively high D^{eff}.

Although Fig. 8 and 9 are for a nonreactive solute, similar results can be obtained for a reactive solute. As long as the assumptions for the stochastic stream tube model and the CDE are different, deviations between the two models like those in Fig. 8 and 9 will exist. When the macroscopic CDE is applied to only BTC, so-called scale-dependent dispersion coefficient (Fried, 1975) may provide a good description of the measured data as shown in Fig. 7. However, the solute distribution for other transport scenarios may not be accurately predicted with the macroscopic CDE. In other words, if D^{eff} has to be modified for each different depth, x, the actual transport model will be different from the CDE.

Calibration and Testing

In an attempt to independently evaluate the stream tube model, we will use the model to simulate nonreactive tracer transport during steady unsaturated flow in a hypothetical random field, which was already observed in a hypothetical numerical experiment by Tseng and Jury (1994) as briefly outlined in the following.

Water flow and solute transport were described by solving the Richards equation and the CDE, respectively. The unsaturated hydraulic functions were described according to van Genuchten (1980). Furthermore, geometric similitude was assumed with a stochastic scaling factor, δ, with variance σ^2_Y = 0.25 where Y = ln 6. The respective horizontal and vertical correlation lengths of 50 and 150 cm are typical for the field (Jury, 1985). Water was applied at a uniform rate, q = 2.16 cm d^{-1}, to the surface of a two-dimensional field with a unit-gradient condition at the bottom. First, a steady flow regime was established with $<\theta>$ = 0.339 and a corresponding CV of 9.4%. Subsequently, solute was applied uniformly for 1 d. The distributions of the total resident concentration were calculated, from which the mean field concentration was obtained by averaging across horizontal transects of the numerical grid. The snapshots of total resident concentrations showed nonuniformity due to lateral variations in the local velocity as

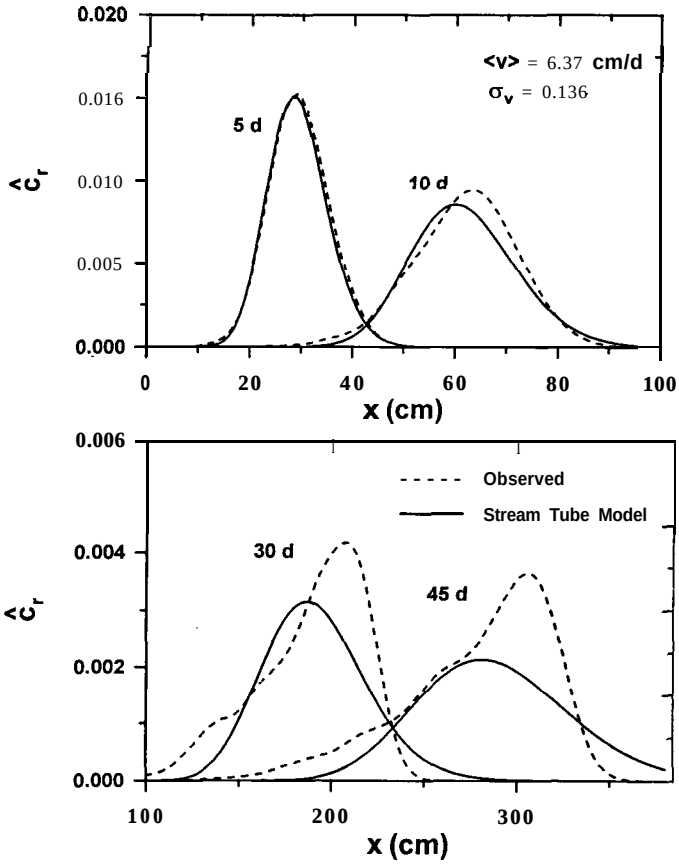

Fig. 10. Observed and predicted field-scale resident concentrations ($\hat{c}_r$) as a function of depth in a hypothetical random field at (a) t = 5 and 10 d, and (b) t = 36 and 45 d (v = pore-water velocity; x = depth).

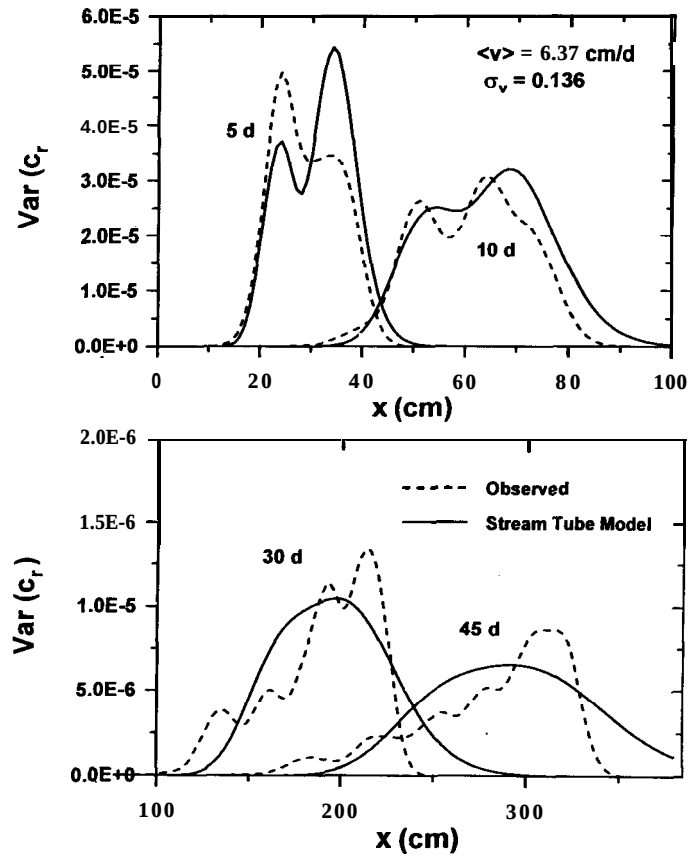

Fig. 11. Observed and predicted variances of the resident concentration, Var (c_r), in the horizontal plane as a function of depth in a hypothetical random field at (a) t = 5 and 10 d, and (b) t = 36 and 45 d (v = pore-water velocity; x = depth).

a result of field heterogeneity [Fig. 3 in Tseng and Jury (1994)].

The field-scale total resident concentration ($\hat{c}_r$) profile at t = 5 d was used to calibrate the standard deviation of the pore-water velocity, σ_v, of the pdf for the stream tube model. A value for σ_v of 0.136 was obtained by the nonlinear least-squares inversion method of Toride et al. (1995). We again assumed θ to be constant due to its relatively low CV. The stream tube model was then used to simulate solute application with $\langle v \rangle$ = 6.37 cm d^{-1}, and $\langle D \rangle$ = 1.6 $cm^2\ d^{-1}$ assuming a constant dispersivity, λ = 0.25 cm. The stream tube model calibrated at t = 5 d was subsequently used for predicting mean concentrations and variances at larger times.

Figure 10 presents $\hat{c}_r$ vs. depth at four selected times. The predicted $\hat{c}_r$ distribution agrees relatively well with the observed distribution. At larger times the observed solutes still remained close to the surface while the concentration front was steep compared with the profile predicted with the stream tube model. Figure 11 shows observed and predicted variances as a function of depth. Although the observed variances after 30 and 45 d fluctuated locally, there seems to be an overall agreement between observed and predicted distributions. The bimodal distribution displayed in Fig. lb was found for both the observed and predicted distributions at 5 and 10 d. The agreement in variance suggests the utility of the stream tube model to simulate transport for this hypothetical heterogeneous field.

Note that the value for σ_v is quite small. For example, Biggar and Nielsen (1976) found that σ_v = 1.25 for ponded infiltration, while Mallants et al. (1996, unpublished data) observed that σ_q = 1.09, where q is the Darcy velocity, in an experiment involving undisturbed l-m-long soil columns.

SUMMARY AND CONCLUSIONS

A stochastic stream tube model for a bivariate lognormal pdf of the pore-water velocity, v, and the distribution coefficient, K_d, was investigated for several types of BVP and IVP problems. Analytical solutions for the equilibrium and nonequilibrium CDE were used for local-scale transport. Solute application at the surface was modeled according to the BVP or the IVP. Although the amount of solute applied across the entire field was the same, the solution to the BVP predicted more spreading in the field-scale resident concentration, $\hat{c}_r$, than the IVP since the amount of solute in each stream tube was proportional to v for the BVP due to the flux-mode injection, while each stream tube contains the same solute mass for the IVP.

The assumption of a lognormal pdf for the standard

conductivity, K_s, with gravitational flow was also discussed in terms of a stochastic pore-water velocity, v. When the recharge rate, r, is larger than K_s, ponding occurs, whereas unsaturated flow occurs in stream tubes where $r < K_s$. Although the stream tube model could be used to describe unsaturated flow with a variable v and θ, the model may become inaccurate since the excess water for stream tubes where $r > K_s$ cannot move into stream tubes with higher K_s. The predicted unsaturated flow will be more uniform than the actual flow. As long as θ is relatively homogeneous compared with the variation in v across the field, the assumption of a lognormal pdf for v with a constant θ appears reasonable.

The variance was evaluated to describe the variation in the local-scale concentration at a particular depth and time in the horizontal plane. An increase in solute spreading because of a higher σ_v, a negative ρ_{vK_d}, or any other reason discussed in Toride and Leij (1996), was accompanied by an increase in the horizontal variation of the concentration. This result indicates that solute spreading in terms of the field-scale mean concentration is the result of a heterogeneous local-scale concentration distribution in the horizontal plane. The effects of correlation between v and K_d on leaching of a reactive solute for the IVP were similar as for the BVP discussed in Toride and Leij (1996), except that the solute spreading associated with a negative correlation is less than that for the BVP. During nonequilibrium adsorption, more time is required to displace solute initially present in the upper part of the soil profile due to slower desorption.

A simplified one-dimensional macroscopic CDE with effective parameters was compared with the stream tube model. The effective parameters for the macroscopic CDE were determined with time moments for the BVP in terms of field-scale flux-averaged concentrations, $\hat{c}_f$. The predicted BTC in terms of $\hat{c}_f$ were similar for the macroscopic CDE and the stream tube model for both nonreactive and reactive solutes. The effective dispersion coefficient, D^{eff}, increased linearly with travel distance. However, the macroscopic CDE with these effective parameters will give different results than the stream tube model for other transport scenarios such as an IVP as well as transport in terms of field-scale resident concentrations, $\hat{c}_r$.

The utility of the stream tube model was finally examined for area-averaged solute transport during steady unsaturated flow in a hypothetical random field. The standard deviation of the pore-water velocity, σ_v, was obtained by fitting the stream tube model to the field-scale resident concentration profile of the numerically generated flow field. The resulting calibrated stream tube model was then used to predict area-averaged transport. The predicted mean concentrations and variances agreed well with observed data. Although the use of a constant θ in case of a lognormally distributed v can only be approximate for unsaturated (heterogeneous) flow, it appears that this approach is reasonable to estimate σ_v and to quantify the heterogeneity of the flow field.

ACKNOWLEDGMENTS

The authors thank Peng-Hsiang Tseng, USDA-ARS, U.S. Salinity Lab., for providing data from the numerical experiment, M.Th. van Genuchten for his review of an earlier version of the manuscript, and R.G. Kachanoski and the anonymous reviewers for their comments.

REFERENCES

Aitcheson, J., and J.A.C. Brown. 1963. The lognormal distribution. Cambridge University Press, London.

Biggar, J.W., and D.R. Nielsen. 1976. Spatial variability of the leaching characteristics of a field soil. Water Resour. Res. 12:78-84.

Bresler, E., and G. Dagan. 1979. Solute dispersion in unsaturated heterogeneous soil at field scale: II. Applications. Soil Sci. Soc. Am. J. 431467472.

Bresler, E., and G. Dagan. 1981. Convective and pore scale dispersive solute transport in unsaturated heterogeneous fields. Water Resour. Res. 17:1683-1693.

Brooks, R.H., and A.T. Corey. 1964. Hydraulic properties of porous media. Hydrology Paper 3. Colorado State Univ., Fort Collins, co.

Burr, D.T., E.A. Sudicky, and R.L. Naff. 1994. Nonreactive and reactive solute transport in three-dimensional heterogeneous porous media: Mean displacement, plume spreading, and uncertainty. Water Resour. Res. 30:791-815.

Dagan, G., and E. Bresler. 1979. Solute dispersion in unsaturated heterogeneous soil at field scale: 1. Theory. Soil Sci. Soc. Am. J. 43:461-467.

Destouni, G., and V. Cvetkovic. 1991. Field scale mass arrival of sorptive solute into the groundwater. Water Resour. Res. 27: 1315-1325.

Fried, J.J. 1975. Groundwater pollution. Elsevier Science, New York.

Jury, W.A. 1985. Spatial variability of soil physical properties in solute migration: A critical literature review. EPRI Topical Rep. EA 4228. Electric Power Inst., Palo Alto, CA.

Jury, W.A., and K. Roth. 1990. Transfer functions and solute movement through soils: Theory and applications. Birkhauser, Basel, Switzerland.

Jury, W.A., and D.R. Scotter. 1994. A unified approach to stochastic-convective transport problems. Soil Sci. Soc. Am. J. 58:1327-1336.

Khan, A.U.H., and W.A. Jury. 1990. A laboratory study of the dispersion scale effect in column outflow experiments. J. Contam. Hydrol. 5:119-132.

Porro, I., P.J. Wierenga, and R.G. Hills. 1993. Solute transport through large uniform and layered soil columns. Water Resbur. Res. 29: 1321-1330.

Sposito, G., W.A. Jury, and V.K. Gupta. 1986. Fundamental problems in the stochastic convection-dispersion model of solute transport in aquifers and fields soils. Water Resour. Res. 22~77-88.

Toride, N., and F.J. Leij. 1996. Convective-dispersive stream tube model for held-scale solute transport: I. Moment analysis. Soil Sci. Soc. Am. J. 60:342-352 (this issue).

Toride, N., F.J. Leij, and M. Th. van Genuchten. 1993. Analytical solutions for nonequilibrium solute transport with first-order decay and zero-order production. Water Resour. Res. 29:2167-2182.

Toride, N., F.J. Leij, and M. Th. van Genuchten. 1995. The CXTFIT code for estimating transport parameters from laboratory and field tracer experiments. U.S. Salinity Lab. Research Rep. 138. Riverside, CA.

Tseng, P-H, and W.A. Jury. 1994. Comparison of transfer function and deterministic modeling of area-averaged solute transport in a heterogeneous field. Water Resour. Res. 30:2051-2063.

van Genuchten, M.Th. 1980. A closed-form equation for predicting the hydraulic conductivity of unsaturated soils. Soil Sci. Soc. Am. J. 44892-898.

van Genuchten, M.Th., and W.J. Alves. 1982. Analytical solutions of the one-dimensional convective-dispersive solute transport equation. USDA Tech. Bull. 1661. U.S. Gov. Print. Office, Washington, DC.